UNIVERSITY OF CALIFORNIA SAN DIEGO

# LARP4 Is an RNA-Binding Protein That Binds Nuclear-Encoded Mitochondrial mRNAs To Promote Oxidative Phosphorylation

A dissertation submitted in partial satisfaction of the requirements for the degree Doctor of Philosophy

in

Biology

by

Benjamin Mark Lewis

Committee in charge:

Professor Tony Hunter, Chair
Professor Gulcin Pekkuranz
Professor Gerald Shadel
Professor Gene Yeo

2022

The Dissertation of Benjamin Mark Lewis is approved, and it is acceptable in quality and form for publication on microfilm and electronically.

University of California San Diego
2022

DEDICATION

This thesis is dedicated to my wife Anne Briggs. Without your love, support, and sense of humor none of this would have been possible.

TABLE OF CONTENTS

LIST OF FIGURES

LIST OF TABLES

## LIST OF ABBREVIATIONS

CDS: Coding DNA/RNA sequence

CRISPR: Clustered regularly interspaced short palindromic repeats

DPBS: Dulbecco's phosphate buffered saline

eCLIP: enhanced crosslinking RNA immunoprecipitation

ENCODE: Encyclopedia of DNA elements, public research project

GO: Gene ontology

KO: Knockout

l2fc: Log2 fold change

MMP: Mitochondrial membrane potential

MOM: Mitochondrial outer membrane

MRP: Mitochondrial ribosome protein

MTS: Matrix targeting sequence

NEMmRNA: Nuclear-encoded mitochondrial mRNAs

OXPHOS: Oxidative phosphorylation

PABP: Poly(A)-binding protein

PAM2: Poly(A)-binding protein interaction motif-2

PAT: Poly(A) tail

PBM: Poly(A)-binding protein interaction motif

PCR: Polymerase chain reaction

OXPP: Oxidative phosphorylation protein

RIR: RACK1 interaction region

RRM: RNA-recognition motif

TBP: TATA-binding protein

TMT: Tandem mass tag

TOM: Translocase of the outer membrane

TMRM: Tetramethylrhodamine, methyl ester

3’UTR: 3 prime untranslated region

ACKNOWLEDGEMENTS

I would like to thank my advisor Tony Hunter for his sponsorship, support, mentorship, and friendship throughout my time in graduate school. I am fortunate and grateful to have joined a lab where the PI creates an egalitarian work environment and encourages researchers to pick their own projects. I would also like to thank my co-advisor Gene Yeo for his support, mentorship and for providing me with access to opportunities and resources. In addition to my thesis advisors, I would like to acknowledge remaining members of my thesis committee Gerald Shadel and Gulcin Pekkuranz for their many insightful and constructive comments that contributed to the success of this work. I would also like thank Immo Scheffler who served on my committee for five years before having to resign for health reasons.

For providing support, ideas and teaching me many techniques throughout my project, I would also like to acknowledge the people of the Hunter Lab including Annie Chou, Huaiyu Sun, Yu Shi, Zheng Wang and Kate (Chae Yun) Cho. In particular, I would like to thank the lab manager of the Hunter lab Jill Meisenhelder, for the extensive training, support and creating a friendly and positive work environment. I am especially grateful for the support and mentorship provided my rotation mentor Xinde Zheng. For their support, I would also like to thank the scientific staff of the Molecular and Cell Biology Lab at the Salk Institute including Justin Zimmermann, Suzy Simon and Mark Schmidit. I would also like thank the members of the Yeo lab for providing scientific ideas and constructive feedback on my lab presentations in particular Stefan Aigner. For computational support I would like acknowledge Brian Yee and Shashank Sathe.

For providing excellent support, training, and access to scientific capabilities, I would like to acknowledge the various scientific core facilities at the Salk Institute. I would like to thank the staff members of the Stem Core Facility for their help. This work was supported by the Flow Cytometry Core Facility (FCCF), of the Salk Institute with funding from with funding from NIH-NCI CCSG: P30 CA014195. I would like to thank the staff of FCCF for technical support and training in particular Carolyn O'Connor, Michelle Liam and Conor Fitzpatrick. This work was supported by the Mass Spectrometry Core of the Salk Institute with funding from NIH-NCI CCSG: P30 014195, an NIH S10 award for metabolic instrumentation: S10 OD021815, and the Helmsley Center for Genomic Medicine. I thank J. Diedrich and A. M. Pinto for technical support. I would like to thank various labs I received reagents from required for this work including Shigeki Miyake-Stoner from the lab of Dr. Clodagh O'Shea for providing the U2OS and HEK293 cell lines as well as Dr. Sandy Mattijssen from the lab of Dr. Richard J. Maraia for providing a LARP4 antibody.

Benjamin Lewis and this work was supported by NIH T32 Cell and Molecular Genetics Training Program (GM007240) as well as grants and awards to Tony Hunter (CA 080100, CA 082683 and CA 242443). This work was supported by grants from the NIH to Gene W. Yeo (U41 HG009889 and HG004659).

Portions of Chapter 2 through 7 are included in a completed manuscript that has been accepted for review at Cell Reports. “LARP4 Is an RNA-Binding Protein That Binds Nuclear-Encoded Mitochondrial mRNAs To Promote Mitochondrial Function” Lewis, Benjamin; Cho, Chae Yun; Yeo, Gene; Hunter, Tony. The dissertation author was the primary investigator and author of this paper.

## VITA

2013 Bachelor of Science in Microbiology and Biochemistry (Double major), California Polytechnic State University, San Luis Obispo, CA

2015 Master of Science in Biology, Specialization: Stem Cell Research and Technology, California Polytechnic State University, San Luis Obispo, CA

2016-2018 Teaching Assistant, Division of Biological Sciences, University of California, San Diego, CA

2022 Doctor of Philosophy in Biology, University of California San Diego, CA

## Publications

"LARP4 Is an RNA-Binding Protein That Binds Nuclear-Encoded Mitochondrial mRNAs To Promote Mitochondrial Function"
*Under review at Cell Reports*
Authors: Benjamin M. Lewis, Chae Yun Cho, Gene W. Yeo, Tony Hunter

*"*Autologous and Heterologous Cell Therapy for Hemophilia B toward Functional Restoration of Factor IX*"*
Cell Reports, May 2018
Authors: Suvasini Ramaswamy, Nina Tonnu, Tushar Menon, Benjamin M. Lewis, Kevin T. Green, Derek Wampler, Paul E. Monahan, Inder M. Verma

"Functional Gene Correction for Cystic Fibrosis in Lung Epithelial Cells Generated from Patient iPSC"
Cell Reports, September 2015
Authors: Amy L. Firth, Tushar Menon, Gregory S. Parker, Susan J. Qualls, Benjamin M. Lewis, Eugene Ke, Carl T. Dargitz, Rebecca Wright, Ajai Khanna, Fred H. Gage, Inder M. Verma

"Drosophila Muller F Elements Maintain a Distinct Set of Genomic Properties Over 40 Million Years of Evolution"
G3-Genes|Genomes|Genetics, May 2015
Authors: Wilson Leung and Participating Students and Faculty of the Genomics Education Partnership

ABSTRACT OF THE DISSERTATION

LARP4 Is an RNA-Binding Protein That Binds Nuclear-Encoded Mitochondrial mRNAs To Promote Oxidative Phosphorylation

by

Benjamin Mark Lewis

Doctor of Philosophy in Biology

University of California San Diego, 2022

Professor Tony Hunter, Chair

The process of protein targeting to mitochondria is complex and relies on both polypeptide and mRNA mediated pathways in a partially redundant manner. Mitochondria associated RNA-binding proteins (RBPs) have emerged as key facilitators of post-transcriptional regulation of nuclear-encoded mitochondrial mRNAs (NEMmRNAs), often by enhancing protein targeting to mitochondria. With only a few examples described in humans, I set out to identify RBPs with a role in post-transcriptional regulation of NEMmRNAs. Through a systematic analysis of the ENCODE collection of eCLIP datasets mapping the binding sites of over a 150 RBPs,

I identified several RBPs with RNA-target sets enriched in NEMmRNAs, of these I selected LARP4 for further analysis. From data produced in multiple human cell lines, I show that the RNA-target set of LARP4 is particularly enriched in mRNAs that encode oxidative phosphorylation proteins (OXPPs) and mitochondrial ribosome proteins (MRPs). I generate LARP4 knockout cell lines to study the consequences of LARP4 depletion. By immunoblot analysis and quantitative proteomics analysis, I show that OXPPs and MRPs are present in reduced abundance in LARP4 knockout cells. Interestingly, cell fractionation experiments showed that the depletion of OXPPS and MRPs was more pronounced in mitochondrial fractions than in whole cell fractions, suggesting defect in protein targeting to mitochondria. Additionally, I show that the depletion of these proteins essential to oxidative phosphorylation has a functional impact on oxidative phosphorylation rates as well as energy dependent cellular processes such as cell proliferation and translation. Furthermore, I show these phenotypes are ameliorated by LARP4 re-expression. Together these data support a novel functional role of LARP4 in post-transcriptionally regulating NEMmRNAs to promote their expression and support oxidative phosphorylation function.

# Chapter 1: Introduction

## 1.1 Protein targeting to mitochondria

Following a single ancient endosymbiotic event, mitochondria of present-day eukaryotes have taken multiple evolutionary paths, but in all cases the vast majority of the ancestral bacterial genome has been either lost or transferred to the host genome and the ancient endosymbiont has long lost its independence (Grey et al., 2001). Expression of the genes required for functional mitochondria is dependent on mRNA transcripts that are transcribed from nuclear-encoded genes, translated by cytosolic ribosomes into proteins and imported into mitochondria. The process of targeting of nuclear-encoded mitochondrial proteins to mitochondria is complex, relies on multiple partially redundant pathways and can occur before (via mRNA targeting), during or after translation in the cytosol (Bolender et al., 2008; Bykov et al., 2020; MacKenzie et al., 2007).

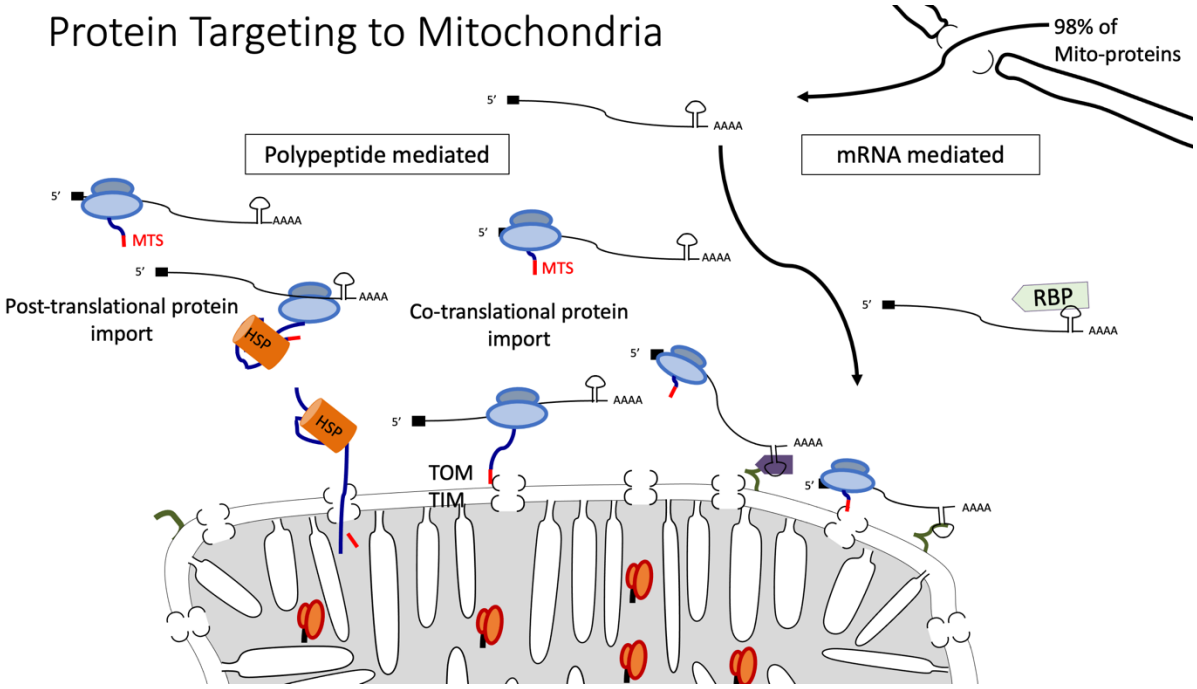


Figure 1. *Diagram protein targeting pathways to mitochondria.*

### 1.1.1 Polypeptide-mediated protein targeting to mitochondria

The most well studied targeting pathway is mediated by polypeptide sorting sequences contained within the proteins that require localization to mitochondria. These cis-acting polypeptide sequences are recognized by other effector proteins that facilitate localization to mitochondria by various mechanisms. There are various types of mitochondrial polypeptide targeting sequences. The canonical matrix-targeting sequence (MTS) is characterized by a N-terminal sequence that forms an alpha-helix secondary structure with positively charged amino acids along one side of the helix axis (Bolender et al., 2008; MacKenzie et al., 2007). The N-terminal MTS is recognized by the outer mitochondrial membrane protein TOM20 which binds the N-terminal amphipathic alpha helix and recruits the peptide to the pore complex of the translocase of the outer membrane (TOM) (MacKenzie et al., 2007; Bolender et

al.2008). In addition to the MTS there are additional signals to target proteins to other mitochondrial compartments (Bolender et al., 2008). There are also mitochondrial targeting sequences located internally within mitochondrial proteins that are recognized by the TOM70 receptor (Bolender et al., 2008; MacKenzie et al., 2007). Furthermore, for some mitochondrial proteins a peptide targeting seqeunce has not been identified suggesting the presence of unique or uncharacterized peptide targeting sequences or possibly a non-peptide mediated targeting mechanism.

When the MTS engages with its mitochondrial receptor before translation is complete and the nascent protein and encoding mRNA are linked via the translating ribosome, the interaction can have the effect of anchoring the encoding mRNA to the outer mitochondrial membrane. In support of this polypeptide-mediated mechanism of mRNA localization, it has been demonstrated in yeast that the association of many nuclear-encoded mitochondrial mRNAs with mitochondria is TOM20 and MTS dependent (Eliyahu et al., 2010).

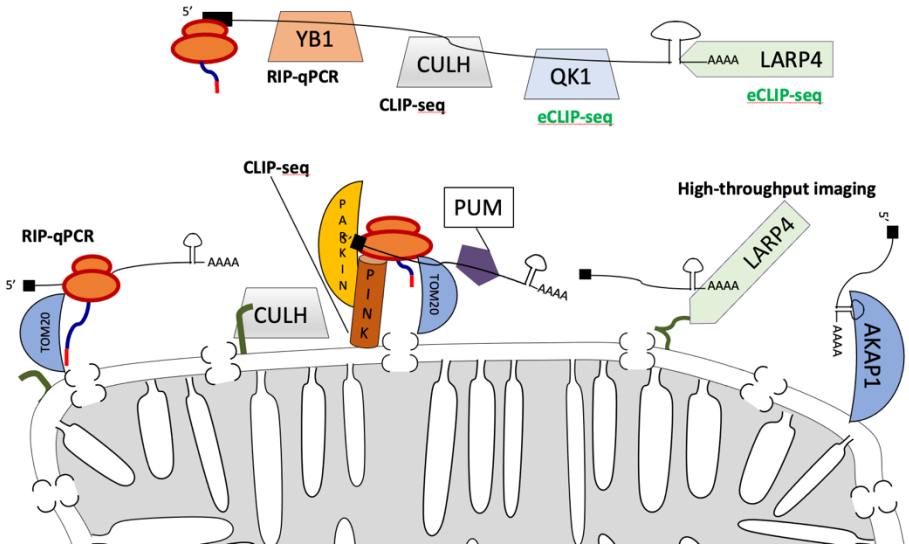


Figure 2. *Diagram mito-associated RBPs in the literature.*

### 1.1.2 mRNA-mediated protein targeting to mitochondria

Several mRNA-mediated targeting pathways for mitochondrial proteins have been described in lower eukaryotes and higher eukaryotes (Bethune et al., 2019; Bykov et al., 2020). These pathways are facilitated by RNA-binding proteins (RBPs) that bind the encoding mRNAs of nuclear-encoded mitochondrial proteins and promote the translation of these mRNAs in the vicinity of mitochondria to facilitate rapid import of the mitochondrial proteins. The mechanisms by which these RBPs promote localized translation are only partially understood, in part because quantitative measurements of the degree of localized translation have been historically difficult to make, and because of this much of the evidence to support this process is indirect. At a minimum the indirect support consists of demonstrated ability of an RBP to bind nuclear-encoded mitochondrial mRNAs (NEMmRNAs) and the demonstrated association the RBP with mitochondria.

One of the best characterized mRNA-mediated targeting pathways is mediated by the RNA-binding protein Puf3p in *Saccharomyces cerevisiae* (hereinafter referred to as yeast). Initially Puf3p was studied in the context of its interaction with the 3'UTR region of a single NEMmRNA (COX17) (Jackson et al., 2004; Olivas et al., 2000). Genome-wide studies showed Puf3p had many NEMmRNAs targets (~250) representing the vast majority (~%86) of the RNA-targets of Puf3p (Gerber et al., 2004). Additionally, a consensus binding motif was identified in the 3'UTR of the majority of Puf3p target RNAs (Gerber et al., 2004). Puf3p was shown to localize to the cytoplasmic face of mitochondrial outer membrane (MOM)

(Garcia-Rodriguez et al., 2007). Using subcellular fractionation of mitochondria-bound and free polysomes it was shown that Puf3p promotes the inclusion of its RNA-targets in mitochondria-bound polysomes and therefore localized translation (Saint-Georges et al., 2008). Furthermore, it was shown in the absence of Puf3p the non-Puf3p target transcripts increased their presence in mitochondria-bound polysomes suggesting that Puf3p binding allows its target mRNAs to out compete other non-target mRNAs for inclusion in the pool of transcripts translated by mitochondria-bound polysomes (Saint-Georges et al., 2008). Puf3p is one of six members of the Pumilio and FBF (PUF) family of RNA-binding proteins present in yeast; in higher metazoans the protein family consists of only two members, in humans Pum1 and Pum2, neither of which have a homologous function to Puf3p in yeast (Quenault et al., 2011). Together these studies have demonstrated that Puf3p is an RBP that primarily binds NEMmRNAs and binds the mitochondrial outer membrane to enhance the association of its target RNAs with mitochondria and prioritize their translation and import into mitochondria (Gerber et al., 2004; Saint-Georges et al., 2008).

In metazoans mRNA mediated protein targeting to mitochondria is more complex involving a more diverse set of RBPs as well as proteins that are not present in yeast. One such pathway involves PINK1, a mitochondrial membrane protein with kinase activity that is stabilized on the MOM of poorly functioning mitochondria with reduced membrane potential (Fallaize et al., 2015). In metazoans, it was demonstrated that PINK1 and its kinase activity promote the mitochondrial localization and translational de-repression of mRNAs encoding nuclear-encoded

respiratory chain complex proteins through the displacement of translational repressors Pum-1 and hnRNP-F (Gehrke et al., 2015).

A conserved metazoan RBP with a similar function to the yeast protein Puf3p is Clueless. The human ortholog of Clueless, CLUH was identified as regulator of mitochondrial biogenesis and was shown to directly bind a subset of nuclear-encoded mitochondrial mRNAs as well as associate with ribosomes (Gao et al., 2014). It was also shown that CLUH depletion results in decreased abundance of the proteins encoded by its target mRNAs (Gao et al., 2014). In both human and *Drosophila* cells, a portion of the cytosolic pool of Clueless was shown to peripherally associate with the MOM, (Gao et al., 2014; Sen et al., 2015), suggesting that Clueless may promote localization of its mRNA-targets to mitochondria. Furthermore, in Drosophila cells, Clueless was shown to preferentially associate with ribosomes present at the mitochondrial surface (Sen and Cox et al., 2016). Together these data, support a model in which Clueless functions to localize its target mRNA to the MOM to promote their localized translation. Future studies should directly show Clueless target mRNA localization to the MOM in a Clueless dependent fashion.

The mitochondria-localized A-kinase-anchoring protein (AKAP1 in humans), binds to and activates protein kinase A (PKA) in response to the second messenger signaling molecule cAMP (Carlucci et al., 2008). In addition to the kinase binding domain, AKAP1 also has an RNA-binding domain which was shown to directly bind structural hairpins in the 3'UTR of two NEMmRNAs and this interaction facilitates the localization of these mRNAs to the MOM and increases the mitochondrial content of the encoded proteins (Ginsberg et al., 2003). Later studies showed that AKAP1 binds

many other NEMmRNAs and through protein-protein interactions recruits other RBPs as well as ribosomes to the MOM to enhance localized translation at the MOM (Gabrovsek et al., 2020). One these RBPs bound by AKAP1 is LARP4, which is the focus of this dissertation. In the Gabrovsek et al., 2020 paper LARP4 was also shown to colocalize with the AKAP1 and the mitochondria in HEK293 cells.

## 1.2 Review of LARP family and LARP4 literature

LARP4 was first identified as one of the La-related proteins (LARPs), each of which is a paralog of the conserved La protein, which functions as a processing chaperone for RNA transcripts produced by RNA polymerase III. The La protein and the LARPs each contain an evolutionarily related RNA-binding protein domain called the La module, which has an evolutionary conserved organization with a La motif followed by an RNA recognition motif (RRM) separated by a linker region (Bousquet-antoneli et al., 2009). The La module of La as well as LARP7 binds the UUU-3'OH present on RNA polymerase III transcripts. The La modules found on the other four LARPs (LARP1, LARP6, LARP4, LARP4B) have diverged in their protein sequence and RNA-binding specificity (Maraia et al., 2017) (Figure 3). The RRM region of the La module is particularly divergent with multiple additional RRM-like motifs present in the LARP family (Bousquet-antoneli et al., 2009; Maraia et al., 2017). Additionally, many of the LARPs have gained additional protein domains to facilitate novel protein-protein interactions (Maraia et al., 2017) (Figure 3).

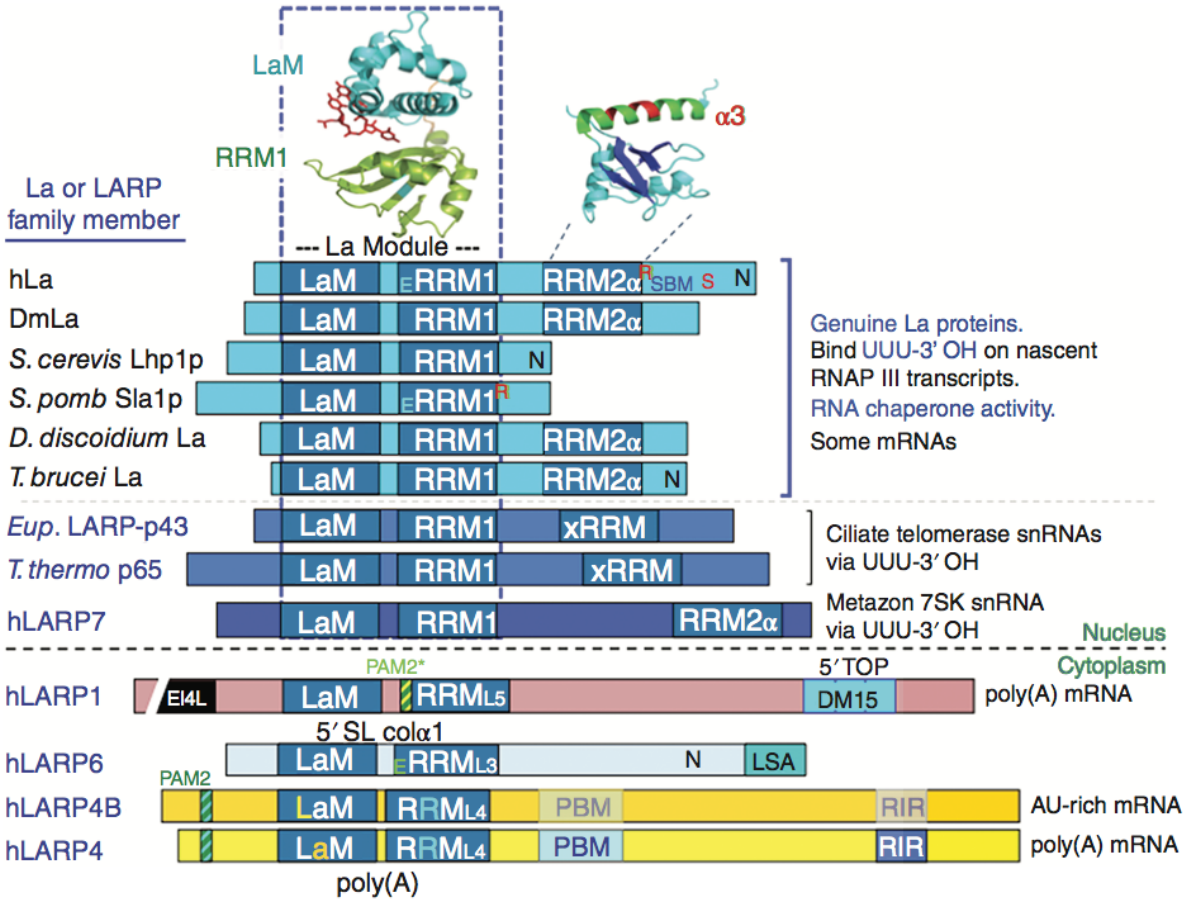


Figure 3. *LA and LA Related Proteins*.
Diagram of the domain structure and organization of selected La proteins and La-related proteins (LARPs). Symbol definitions: PAM2: Poly(A)-binding protein interaction motif 2; LaM: La motif; $RRM_{L4}$: RNA Recognition motif – like variant 4; PBM: Poly(A)-binding protein binding motif; RIR: Rack1 interaction region. Figure is a direct reprint of from Maraia et al., 2017.

### 1.2.1 LARP4 domains and RNA interactions

LARP4 has five characterized protein domains. These include the La motif and RRM-like motif that make up the La module of LARP4, two domains that interact with the poly-A binding protein (PAM2 and PBM) and a C-terminal domain that interacts with RACK1 (RIR) (Maraia et al., 2017) (Figure 3). Through polysome analysis, LARP4 was shown to integrate into actively translating polysomes (Yang et al., 2011). Through a yeast 2-hybird screen, LARP4 was shown to interact with the

RACK1 protein (Yang et al., 2011). RACK1 is protein that stably associates with the 40S ribosome subunit and acts as a scaffold for interactions with other proteins (Adams et al., 2011). LARP4 contains a variant PAM2 motif at positions 13-22 that directly binds the MLLE domain present in the family of poly-A binding proteins (PABPs) and this motif contributes significantly to LARP4 polysome association (Yang et al., 2011). This variant motif differs from the consensus PAM2 motif, SXLNXNAXXF in that it contains a tryptophan in place of the otherwise invariant phenylalanine (F) at position 10 (Yang et al., 2011). In addition to the PAM2 motif, a second region of LARP4 (288-358) promotes binding to PABPs and polysomes and is referred to as the PABP interaction motif (PBM) (Figures 3 and 4) (Yang et al., 2011). In addition to the protein interaction domains, the RNA-binding domains of the La-module were also shown to contribute to polysome association (Yang et al., 2011). LARP4 was also shown to co-localize with stress granules (Yang et al., 2011). Proximity-based labeling proteomics also identified LARP4 as a stress granules component (Markmiller et al, 2017). LARP4 has five major isoforms including the full-length isoform (A), an isoform (B) missing a single amino acid at the first splice site, an isoform (F) missing a short internal segment (374-445) following the PBM region, an isoform (E) missing the C-terminal region (445-724) and an isoform (H) missing the first half and of the N-terminal region (1-70) including the PAM2 motif as well as the C-terminal region (445-724).The function of these alternative isoforms is unclear (Figure 4).

LARP4's RNA interactions are thought to be facilitated by both direct interactions via RNA-binding protein domains and indirect interactions via protein-

protein interactions with other RNA associated proteins. Upon initial characterization, LARP4 was shown to bind directly to poly-A RNA nucleotides through the La-module containing N-terminal domain (1-287) (Yang et al., 2011). Later studies showed that LARP4's direct interaction with poly-A RNA was primarily driven by its variant PAM2 motif and the surrounding unstructured N-terminal region (1-111) with the La-module (112-287) only playing a minor role (Figure 4) (Cruz-Gallardo et al., 2019).

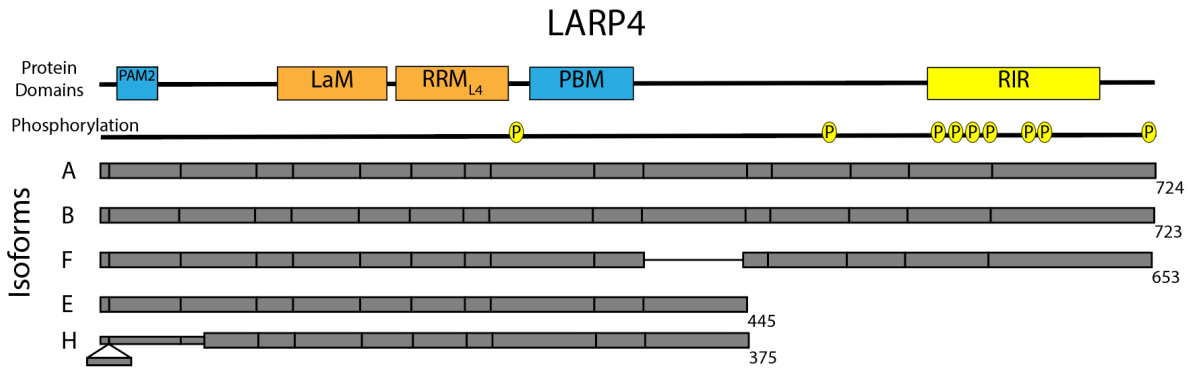


Figure 4. *LARP4 isoforms and domains diagram.*
NCBI entry for Gene ID: 113251 used to generate this diagram
https://www.ncbi.nlm.nih.gov/gene?Db=gene&Cmd=DetailsSearch&Term=113251

### 1.2.2 LARP4 RNA-related function

Evidence suggests that LARP4 has functional roles in multiple aspects of RNA metabolism. Multiple lines of evidence support LARP4 regulating translation. In addition to its direct interactions with translational proteins (PABP and RACK1) LARP4 knockdown has direct effects on translation. Upon LARP4 knockdown, polysome profile analysis shows a decrease in polysome abundance relative to monosome abundance suggesting decreased translation initiation; additionally reduced $^{35}$S-methionine incorporation was observed in pulse chase assays suggesting a global reduction in cellular protein synthesis (Yang et al., 2011). LARP4

is also a mRNA stabilization factor. Initially LARP4 overexpression was shown to stabilize a reporter mRNA and to a lesser extent stabilize endogenous mRNA transcripts (Yang et al., 2011). Later studies demonstrated that LARP4 plays a functional role in maintaining poly-A tail (PAT) length, likely through competition with deadenylases for PABP binding sites (Mattijssen et al., 2017; Mattijssen et al., 2020). Recently, LARP4 was reported to be recruited to the mitochondrial surface through an interaction with PKA adaptor protein AKAP1, which also functions as an RNA-binding protein (Gabrovsek et al., 2020). Those authors proposed that once recruited to the mitochondrial surface LARP4 acted as a general translation factor to facilitate local translation of mitochondrial mRNAs bound by AKAP1 at the mitochondrial surface (Gabrovsek et al., 2020). However, LARP4's RNA-targets were not determined.

Chapter 2: Identification and analysis of the RNA-targets of LARP4

With the goal of identifying human RBPs with a novel role in mitochondrial biology, I made use of the ENCODE collection of 223 enhanced CLIP-seq (eCLIP) datasets profiling 150 RBPs in K562 and HepG2 cell lines in a standardized workflow (Van Nostrand et al, 2020). Through a systematic computational analysis of these eCLIP datasets, several RBPs with RNA-target sets enriched for nuclear-encoded mitochondrial mRNAs (NEMmRNAs) were identified. Of these NEMmRNA-enriched RBPs, LARP4, a La-related RBP, was selected for further study, due to an enrichment for RNA-targets encoding oxidative phosphorylation proteins (OXPPs) and mitochondrial ribosome proteins (MRPs) as well as the lack of previous reports linking LARP4 to mitochondria (Figure 5).

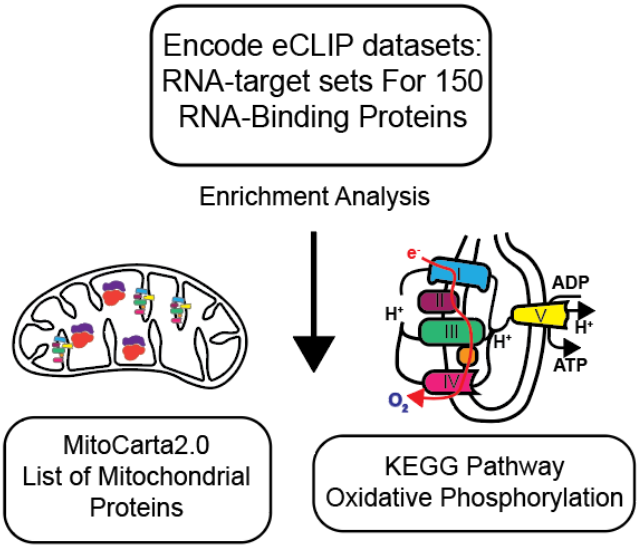


Figure 5. *Diagram of ENCODE search for mito-associated RBPs*.

## 2.1 Mitochondrial-associated RNA-binding proteins found in ENCODE data

The ENCODE consortium has recently made publicly available the RNA-binding profiles of hundreds of RNA-binding proteins (RBPs). This was done by

performing the eCLIP-seq assay for 150 RBPs in two human cell lines (HepG2 hepatocellular carcinoma and K562 erythroleukemia) for each RBP in duplicates (Van Nostrand et al, 2020). To identify additional RBPs involved in post-transcriptional regulation of NEMmRNAs, I performed a systematic computational analysis of the ENCODE collection of eCLIP datasets. I searched these datasets to identify RBPs with RNA-target sets that are statistically enriched for mRNAs encoding either proteins localized to mitochondria (Mitocarta_2.0) or proteins specifically involved in oxidative phosphorylation (KEGG OXPHOS pathway) (Figure 5). This approach led to the identification of several RBPs with a preference for binding NEMmRNAs including: LARP4, DDX3X, RPS3, SUB1, PABPC4, YBX3 and several others (Figures 6A and 6B).

Among them LARP4 stood out as one of the most enriched. Compared to the other ENCODE datasets, the RNA-target set of the LARP4 HepG2 dataset was third most enriched for mitochondrial targets and was more enriched for OXPHOS targets than any other dataset. The LARP4 K562 dataset was also enriched for OXPHOS targets but to a lesser degree. I then performed an independent LARP4 eCLIP sequencing experiment in the human embryonic kidney cell line HEK293 (see Figure 12A). I performed a similar enrichment analysis and discovered an even greater enrichment for RNA-targets encoding mitochondrial protein or oxidative phosphorylation proteins than observed in any of the other ENCODE eCLIP datasets available at the time (Figures 6A and 6B).

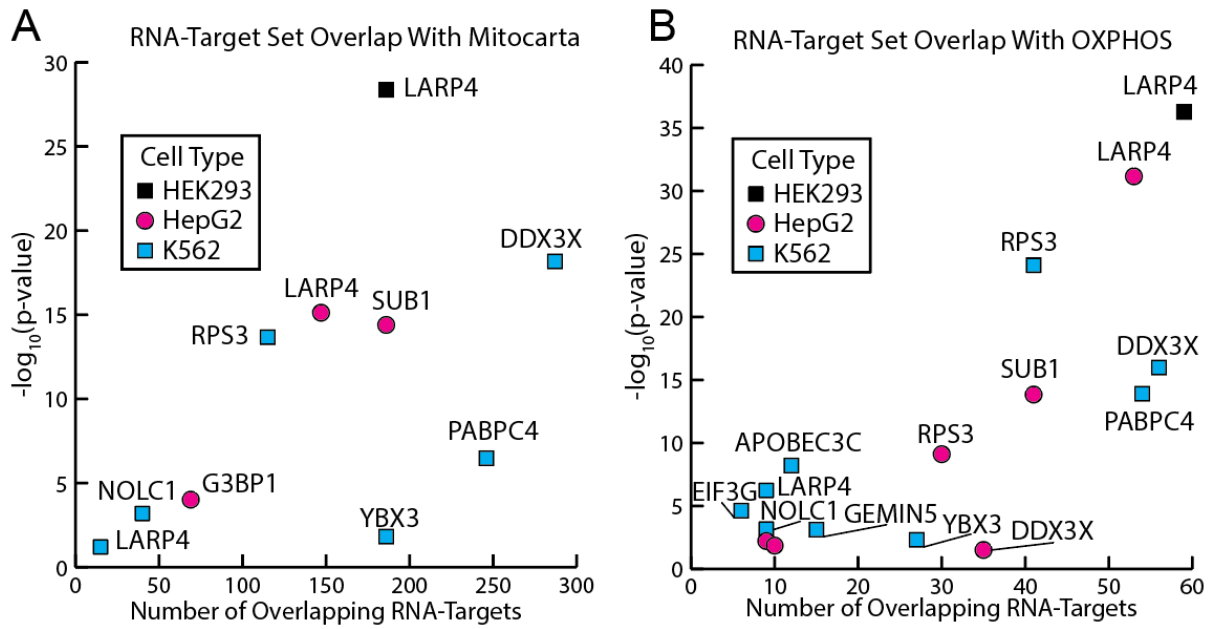


Figure 6. *RNA-target set overlap analysis results for mitochondrial genes or OXPHOS genes.*
(A) Enrichment analysis results for RNA-target set (eCLIP data) overlap with mitochondrial genes. The hypergeometric test for significance of overlap for each RBP dataset is plotted on the y-axis and the number of overlapping targets is plotted on the x-axis. RBPs with significant overlap (p-value≤0.05) with LARP4-K562 also shown (p-value=O.06). (B) Enrichment analysis results for RNA-target set (eCLIP data) overlap with proteins in the KEGG oxidative phosphorylation pathway (HSA_00190). Only RBPs with significant overlap (p-value≤0.05) are shown.

## 2.2 RNA-target sets of the three LARP4 eCLIP datasets

Three LARP4 eCLIP datasets were available for analysis at the time of writing, two generated by the ENCODE consortium produced in HepG2 cells and K562 cells and one additional dataset produced in HEK293 cells generated by author of this dissertation. For each dataset lists of genes that encode RNA-targets of LARP4 were generated by including each gene containing with an eCLIP peak that met the following criteria: log2 fold change (CLIP-IP/Input) greater than 4 and -log10(pValue) greater than 7. This is a more conservative threshold filter for a significant eCLIP

peak and results in a smaller list of RNA-targets, than the less conservative baseline threshold filter (l2fc>3 and -log10pvalue>3).

Overlap between these gene-target lists was greatest between the LARP4 eCLIP dataset generated from HEK293 (713 targets) and HepG2 cells (674 targets), which are both of epithelial origin, with 347 overlapping targets (Figure 7A). The K562 cell dataset generated substantially fewer overall gene-targets (85 targets) possibly due to a less than optimal UV-crosslinking or immunoprecipitation during the eCLIP procedure or cell-type specific differences (Figure 7A). The proportion of RNA-targets that encode mitochondrial proteins for each dataset are 26% (186/713) for the HEK293 dataset, 22% (147/664) for the HepG2 dataset and 18% (15/85) for K562 dataset. The overlap between gene targets of each LARP4 eCLIP dataset was even greater when only considering eCLIP targets that are also NEMmRNAs (Figure 7B).

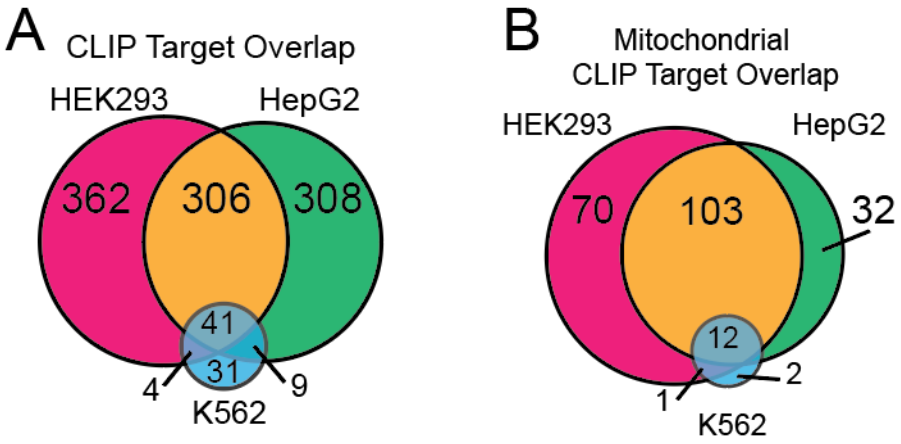


Figure 7. *Overlap between LARP4 eCLIP datasets.*
(A) Venn diagram showing the overlap between gene-target list of each of the three LARP4 eCLIP datasets from HEK293, HepG2, K562 cells. (B) Venn diagram showing the overlap between gene-targets that are also mitochondrial genes.

## 2.3 Gene ontology analysis of three data sets

Gene ontology (GO) analysis was performed on the three LARP4 eCLIP datasets lists using the Metascape method (Figures 8A, 8B and 8C) (Zhou et al., 2019). For each dataset, gene-target lists were generated using the same criteria as above and dataset specific background gene lists were generated from the corresponding control eCLIP input libraries by including all genes with at least 5 reads. Oxidative phosphorylation (GO: 0006119) was the most enriched gene ontology term for both the HEK293 and HepG2 datasets (Figures 8A and 8B) and one of the top three terms for the analysis performed on the K562 eCLIP dataset (Figure 8C). There were also several terms associated with oxidative phosphorylation enriched in both HEK293 and HepG2 datasets such as proton transmembrane transport and respiratory chain complex I (Figures 8A and 8B). Terms associated with coping with the toxic reactive oxygen species generated by oxidative phosphorylation were also present in the group of enriched GO terms such as detoxification of reactive oxygen species (HEK293), cellular response to chemical stress (HEK293 and HepG2) and cellular oxidant detoxification (HepG2).
The translation (RHSA:72766) gene ontology term which includes proteins that make up the cytosolic ribosome as well as the mitochondrial ribosome was the second most enriched term in both the HEK293 and HepG2 cell eCLIP datasets. This enrichment for translational genes was also substantial when compared to other RBPs in the ENCODE dataset collection with the RNA-target sets all three LARP4 eCLIP datasets ranking among the top ten most enriched for translational targets (Figure 9B). Furthermore, mitochondrial translation elongation (RHSA-5389840), a

term that was primarily composed of genes that encode mitochondrial ribosome proteins (MRPs), was also a top gene ontology term of both the HEK293 and HepG2 cell eCLIP datasets (Figures 8A and 8B). These gene ontology results show a strong association between the RNA-targets of LARP4 and the process of oxidative phosphorylation, with enriched gene ontology terms composed of proteins directly involved in oxidative phosphorylation, proteins that support the biogenesis of the OXPHOS machinery (MRPs) and proteins that help cope with the oxidative stress associated with OXPHOS.

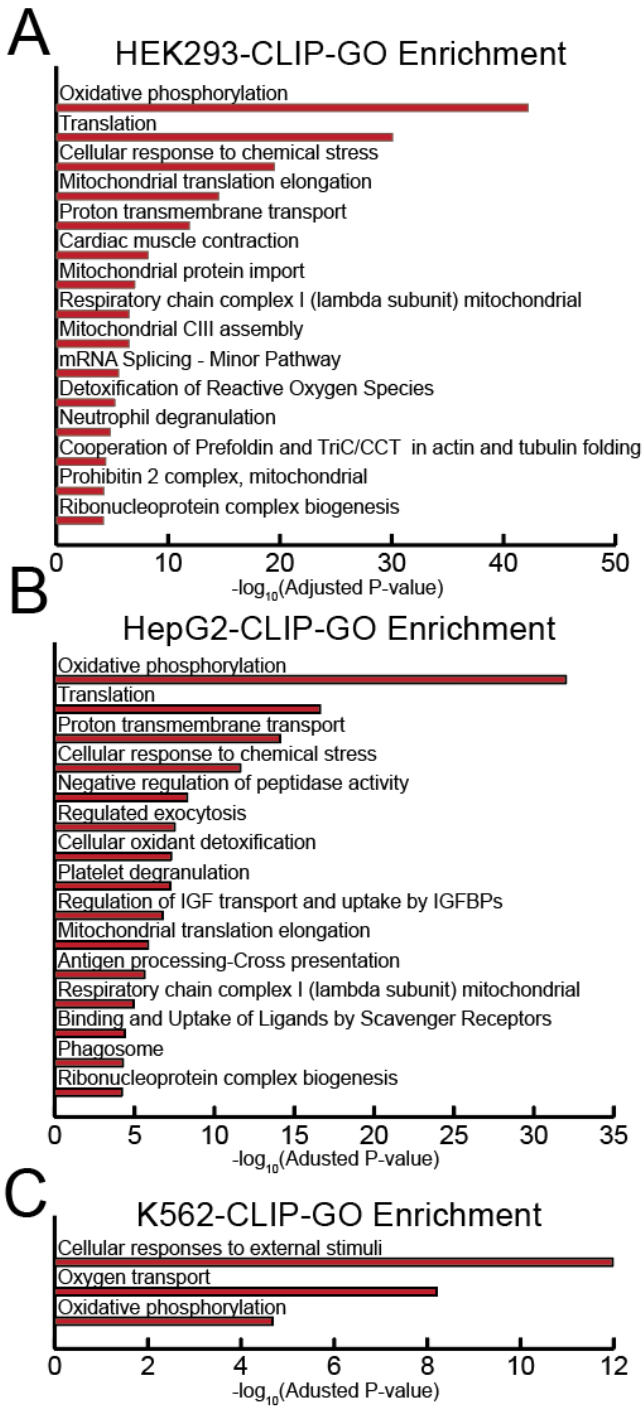


Figure 8. *Gene ontology analysis of LARP4 RNA-sets from eCLIP datasets.*
(A-C) Metascape gene ontology analysis performed on the three LARP4 eCLIP-seq data sets from (A) HEK293, (B) HepG2, (C) K562 cells.
Gene-target lists of each eCLIP-seq dataset are defined as genes encoding an mRNA containing at least one eCLIP peak that passes significance thresholds (-log10Pvalue > 7, log2foldchange (IP/input) > 4 ).

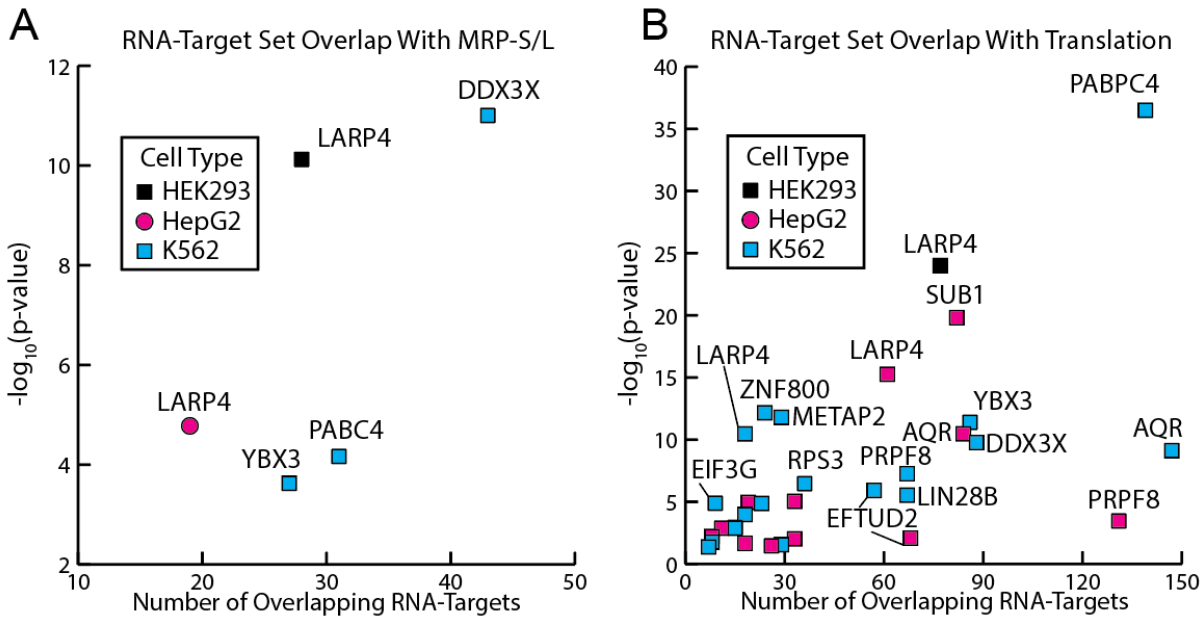


Figure 9. *RNA-target set overlap analysis results for set of mitochondrial ribosome proteins (MRP-S/L) or set of translations genes.*
(A) Enrichment analysis results for RNA-target set (eCLIP data) overlap with mitochondrial ribosome proteins (MRP-S/L) defined by gene ontology term GO_0005761. Only RBPs with significant overlap (p-value<0.05) are shown.(B) Enrichment analysis results for RNA-target set (eCLIP data) overlap with proteins in the Translation pathway (R_HSA_72766). Only RBPs with significant overlap (p-value<0.05) are shown.

2.4 mRNA-targets encoding mitochondrial ribosome proteins (MRPs)

Because the gene ontology analysis found that genes in the mitochondrial translation elongation term to be enriched in both the HEK293 and the HepG2 cell eCLIP datasets, I sought to directly test if transcripts encoding mitochondrial proteins were enriched in the LARP4 HEK293 eCLIP dataset. Using the same enhanced significance criteria for eCLIP peaks (l2fc>4 and -log10pvalue>7) as used for the gene ontology analysis, there were LARP4 peaks present in 28 out of the 89 genes that encode for mitochondrial ribosome proteins (MRPs) as defined by the GO:OOO5761 gene ontology term. At the less conservative baseline threshold for eCLIP targets (l2fc>3 and -log10pvalue>3) the number of MRPs present in LARP4

RNA-target set increases to 52. The hypergeometric significance test was used to confirm that this number of MRP targets in the RNA-target set of LARP4 represents a significant (p-value=6e- 11) overrepresentation (Figure 12C). I then looked for overrepresentation of mRNAs encoding MRPs in the RNA-target sets of other RBPs in the ENCODE eCLIP dataset collection for comparison. Using the hypergeometric significance test, I only found 4 ENCODE eCLIP datasets with RNA-target sets in which mRNAs encoding MRPs were significantly overrepresented, of these the LARP4 HepG2 dataset was the 2$^{nd}$ most enriched (Figure 9A). The RNA-target set of the LARP4 HEK293 eCLIP dataset was even more enriched for MRPs than the HepG2 dataset (Figure 9A). LARP4 binding profiles across two representative transcripts encoding MRPs are shown in Figure 10. Together these data show that mRNAs encoding MRPs are statistically enriched in the RNA-target sets of LARP4 eCLIP datasets from multiple cell lines, suggesting the possibility that LARP4 regulates these mRNAs in some way.

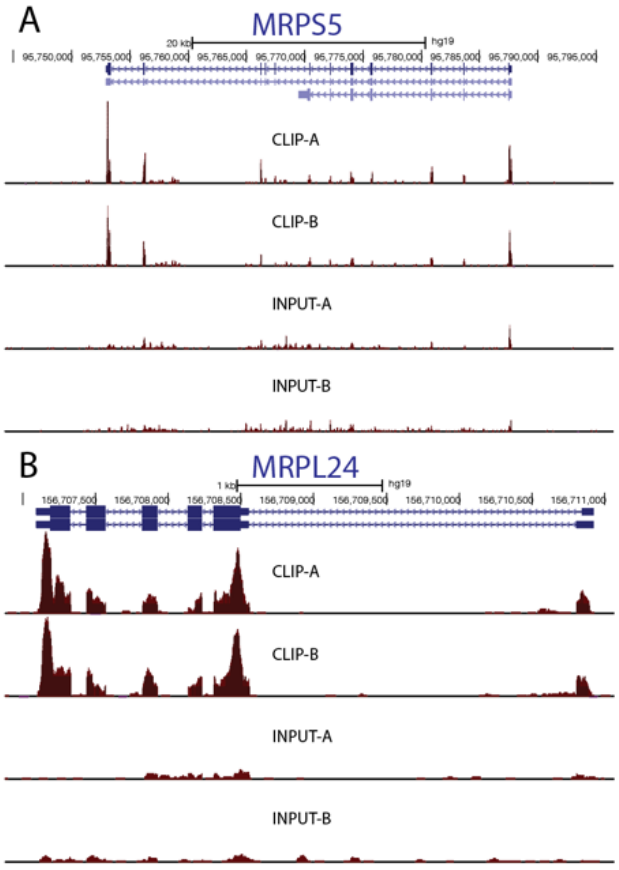


Figure 10 *Genome browser tracks of LARP4 target mitochondrial ribosome proteins.* LARP4 eCLIP data (HEK293) showing the gene locus for (A) MRPS5 and (B) MRPL24. The read density plots for the two eCLIP IP library replicates (CLIP-A and CLIP-B) are shown above the two size matched inputs control library replicates (INPUT-A and INPUT-B).

## 2.5 mRNAs targets encoding oxidative phosphorylation proteins (OXPPs)

Within the RNA-target set of LARP4, mRNAs encoding oxidative phosphorylation proteins (OXPPs) were the most robustly overrepresented group of functionally related targets. All three LARP4 eCLIP datasets from separate cells lines showed a significant overrepresentation of OXPHOS targets in their RNA-target sets. The LARP4 RNA-target sets from the HEK293 and HepG2 eCLIP datasets were more enriched for mRNAs encoding OXPPs than any other RNA-targets set found in the ENCODE collection of eCLIP datasets profiling 150 RBPs (Figure 6B). The HEK293 dataset was the most enriched (p-value=$5e^{-37}$) of all datasets analyzed

(Figures 6B and 12B). LARP4 binding profiles across 3 representative transcripts encoding OXPPs are shown in Figure 11. These data from multiple cell lines indicate that LARP4 has preference for binding mRNAs encoding OXPPs, implicating LARP4 in some type of regulation of these mRNAs.

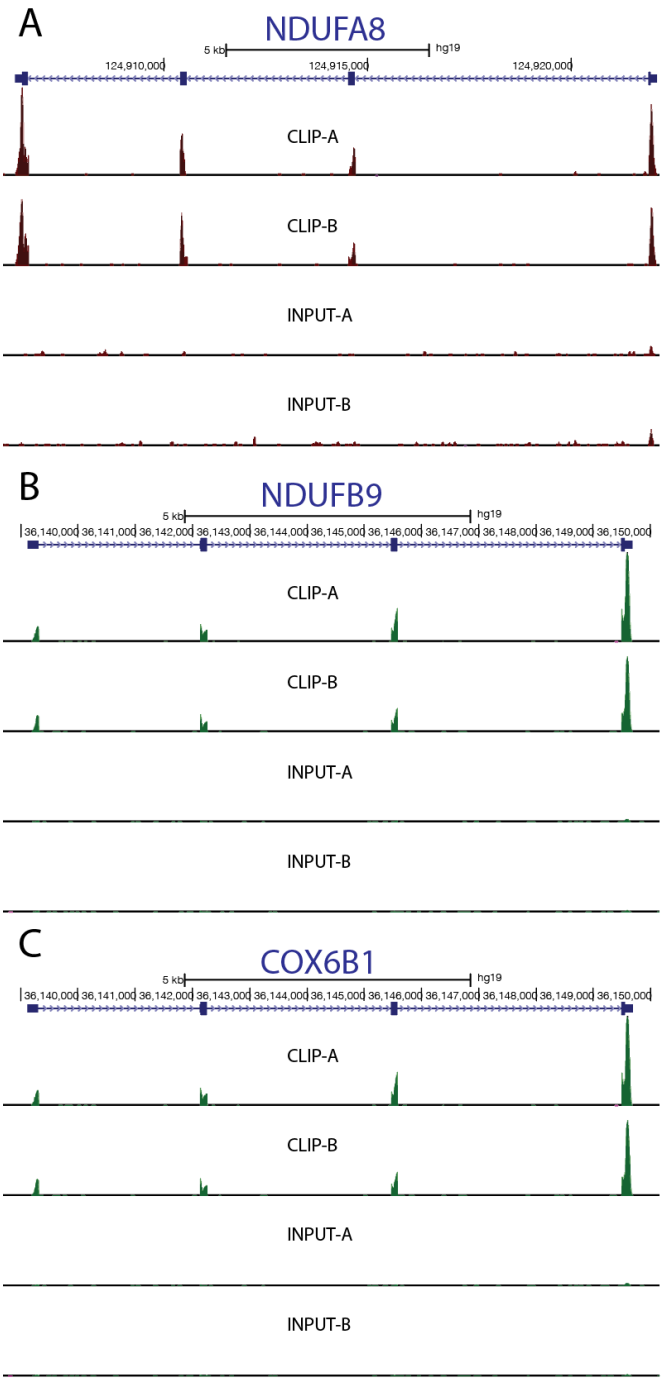


Figure 11. *Genome browser tracks of LARP4 target OXPHOS proteins.*
LARP4 eCLIP data (HEK293) showing the gene locus for (A) NDUFA8, (B) NDUFB9 and (C) COX6B1. The read density plots for the two eCLIP IP library replicates (CLIP-A and CLIP-B) are shown above the two size matched inputs control library replicates (INPUT-A and INPUT-B).

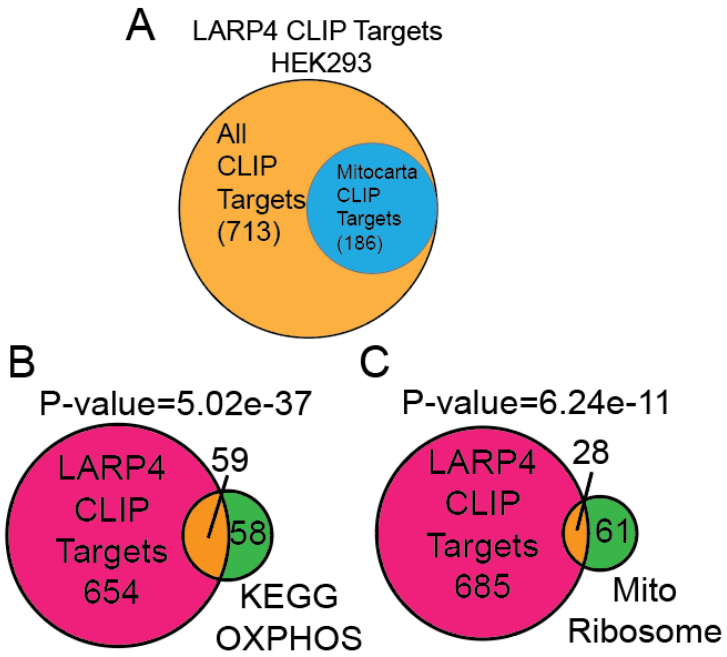


Figure 12. *Enrichments of functional gene groups in LARP4 RNA-targets.* (A) Venn Diagram showing the proportion of LARP4 CLIP targets that encode for mitochondrial proteins. (B) Venn diagrams showing the overlap HEK293's LARP4 eCLIP gene-target list with oxidative phosphorylation genes (HSA_00190). (C) Venn diagrams showing the overlap HEK293's LARP4 eCLIP gene-target list with mitochondrial ribosome proteins (GO:OOO5761).

2.6 MOTIFF analysis / binding profile

How LARP4 achieves its RNA-target specificity is not fully understood. Using the HEK293 eCLIP dataset, I performed k-mer analysis to identify possible linear sequence motifs in LARP4's RNA-target sets. While robust k-mer motifs were not identified, there was a weak degenerate C-rich motif present within the LARP4 peaks present in 3'UTRs of target genes (Figure 13). LARP4's eCLIP data shows that LARP4 coats many of its target mRNAs from CDS to 3'UTR with larger peaks often observed near the start and stop codons (Figures 10 and 11). LARP4 contains both RNA-binding domains (La-module, RRM, and n-terminal PAM2 region) and protein interaction domains that interact with other RBPs or RNA-associated proteins such as Poly-A binding proteins (PABPs) and RACK1 (Maraia et al., 2017; Cruz-Gallardo

et al., 2019). It is possible that LARP4's RNA-target specificity is achieved through a cooperative mechanism involving both its RNA-binding domains and its protein interaction domains. Although linear motifs were not identified, it is also possible that LARP4 recognizes a structural RNA motif which plays a role in defining its RNA-target specificity. Future studies should test hypothesis using RNA structure prediction methods.

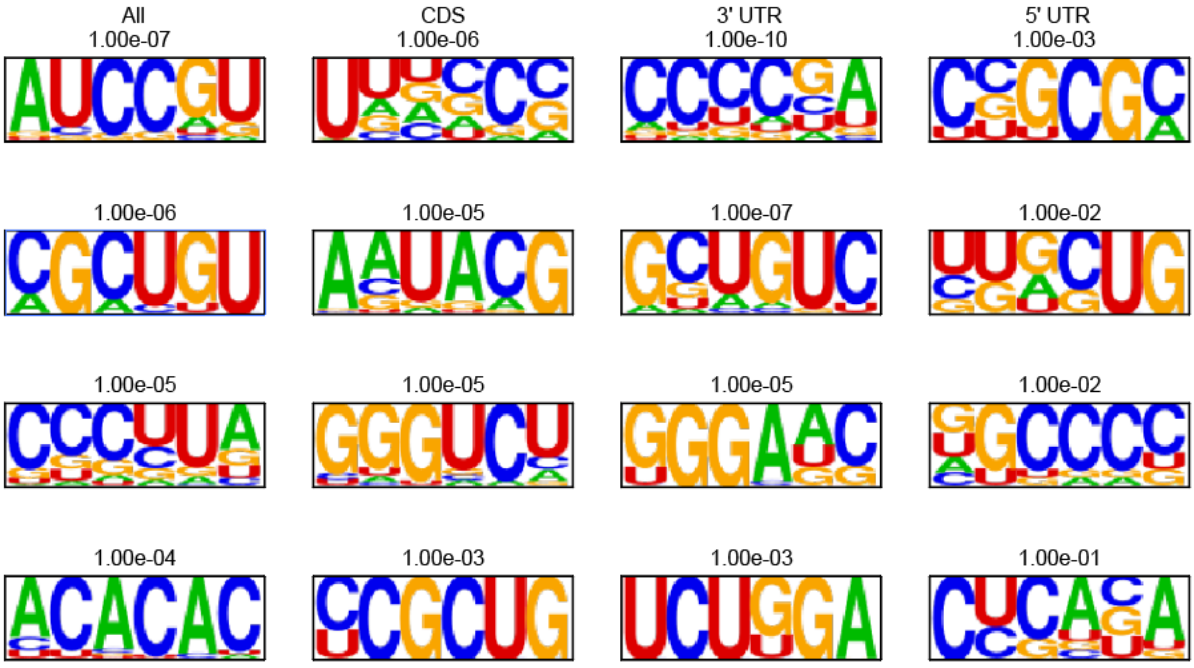


Figure 13. LARP4 motif analysis - HEK293 eCLIP dataset
Motif analysis performed on the HEK293 eCLIP dataset. Peak regions were filtered for peaks with -log10Pvalue > 3, log2foldchange (IP/input) > 4.

## 2.7 Chapter 2 conclusion

Together the data present in this chapter identify LARP4 as an RBP with a robust preference for binding functionally related nuclear-encoded mitochondrial mRNAs (NEmRNAs) in multiple cell lines. Of these NEmRNAs targets, mRNAs encoding OXPPs as well as MRPs are particularly overrepresented (Figures 12B and 12C). Strikingly the RNA-target set of LARP4 is more enriched in mRNAs encoding

OXPPs than any other of the 223 RNA-target sets analyzed for comparison. Other gene ontology terms overrepresented in RNA-target sets of LARP4 are composed of proteins that functionally support the OXPHOS pathway e.g., mitochondrial translation elongation or help mitigate the cytotoxic chemical stresses produced by the OXPHOS pathway e.g., cellular response to chemical stress and detoxification of Reactive Oxygen Species (Figures 12C, 8A, and 8B). These data strongly suggest LARP4 plays some functional role in regulating the OXPHOS pathway.

Portions of Chapter 2 are included in a completed manuscript that has been accepted for review at Cell Reports. “LARP4 Is an RNA-Binding Protein That Binds Nuclear-Encoded Mitochondrial mRNAs To Promote Mitochondrial Function” Lewis, Benjamin; Cho, Chae Yun; Yeo, Gene; Hunter, Tony. The dissertation author was the primary investigator and author of this paper.

Chapter 3: Loss of LARP4 disrupts protein levels without affecting mRNA abundance of mitochondrial targets

To study the functional consequences of LARP4 depletion, CRISPR knockout (KO) cell lines were generated in HEK293 and U2OS cell lines. Protein levels of select RNA-targets of LARP4 were measured by immunoblot and corresponding mRNA levels measured by RT-qPCR.

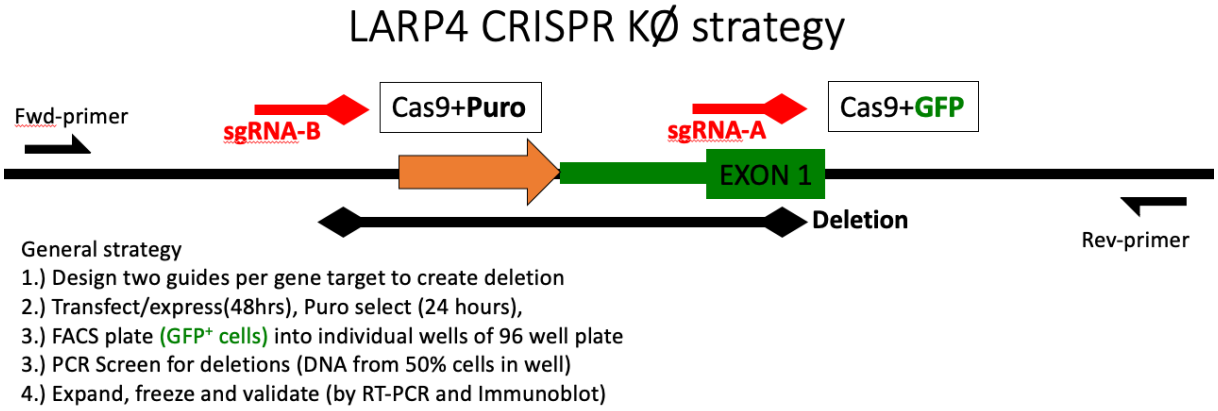


Figure 14. *LARP4 CRISPR knockout strategy.*

## 3.1 Generation and validation of LARP4 CRIPSR knockout cell lines

Genome editing was performed using the CRISPR/Cas9 system to disrupt LARP4 expression (Figure 14). The CRISPR/Cas9 system was introduced into cells by transient transfection and then single cells expanded to generate clonal sub-clone cultures which were screened to identify knockout lines. To enable screening of the sub-clone cultures by simple PCR, two locations at the LARP4 genomic locus were targeted with Cas9 such that a small deletion would be a possible outcome following double stranded breaks at both target sites. Sub-clones were then screened by PCR using primers flanking the two cut sites (Figure 15A). Sub-clones showing evidence of a deletion at one or more of the 3 alleles present in these transformed cells were expanded and further screened by immunoblot to identify clones in which LARP4

protein expression had been disrupted (Figure 15B). The knockout lines selected for functional studies were further validated by performing Sanger sequencing of the LARP4 genomic locus (Figure 15D).

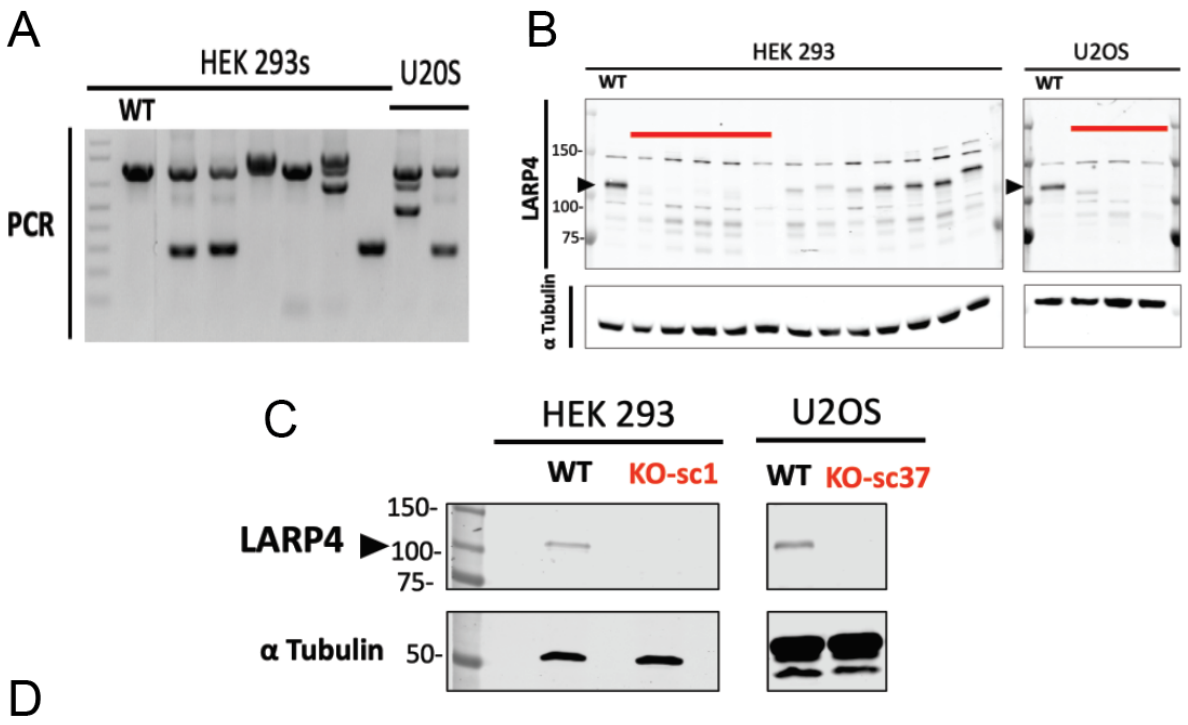


D

HEK293 WT and LARP4-KO-sc1

CRISPR-B:-CGACATGTTGCTTTTCGTGG-PAM
WT:GAGGACGACATGTTGCTTTTCGTGGAGGTGAGTGCATTATGCTAGTCTC - Wild type sequence
A:----------TGGAGGTGAGTGCATTATGCTAGTCTC - Deletion of first exon and Promotor
B:--GAGGACGACATGTTGCTTTTTT----------TTATGCTAGTCTC - Insetion and Deletion in first Exon
C:--GAGGACGACATGTTGCTTTTCG---------- AGTGCATTATGCTAGTCTC - Deletion in first exon

U2OS WT and LARP4-KO-sc37

CRISPR-B:-CGACATGTTGCTTTTC--GTGG-PAM
WT:GAGGACGACATGTTGCTTTTC--GTGGAGGTGAGTGCATTATGCTAGTCTC - Wild type sequence
A: ----------GTGAGTGCATTATGCTAGTCTC - Deletion of first exon and Promotor
B: ----------GTGAGTGCATTATGCTAGTCTC - Deletion of first exon and Promotor
C:--GAGGACGACATGTTGCTTTTCGGTGGAGGTGAGTGCATTATGCTAGTCTC - Single base pair insertion in CDS

Figure 15. *DNA gel from PCR screen of DNA from CRISPR treated subclones.* (A) Representative DNA gel from PCR screen of DNA from subclones recovered after CRISPR/Cas9 treatment. (B) Immunoblot screen of selected subclones. (C) Immunoblot validation of knockout subclones selected for functional studies. (D) Summary of CRISPR cut sight analysis by Sanger sequencing of knockout subclones selected for functional studies.

## 3.2 Immunoblot analysis of selected lines

Because mRNAs encoding OXPPs and MRPs were particularly enriched in LARP4's RNA target set, expression levels of representative proteins from these protein complexes were characterized by immunoblot analysis (Figures 16A,16B,17A and 17B). Based on the strong LARP4 binding to their encoding transcripts NDUFA8, NDUFB9, COX5B and COX6B1 were selected as representative OXPPs; MRPS5 and MRPL24 were selected as representative MRPs. The TATA-Box binding protein (TBP) was included as a non-LARP4 target loading control. Biological replicate samples of whole cell extracts were collected from knockout cell lines and their respective wild-type parental lines for analysis. Antibody signals were normalized with a quantitative total protein stain and replicate averages quantified (Figures 16B and 17B). Samples from HEK293$^{LARP4-/-}$ KO cells (Figures 16A and 16B) showed a significant reduction in protein expression levels of multiple OXPPs (NDUFA8: KO/WT=0.67, NDUFB9: KO/WT=0.74 and COX6B1: KO/WT=0.16) and multiple MRPs (MRPS5: KO/WT=0.52 and MRPL24: KO/WT=0.72). Parallel analysis of samples from U2OS$^{LARP4-/-}$ KO cells (Figures 17A and 17B) showed protein levels were reduced in most cases (NDUFA8: KO/WT=0.83, COX5B: KO/WT=0.48, COX6B1: KO/WT=0.88 and MRPS5: KO/WT=0.75 ), but significantly increased in one case (MRPL24: KO/WT=1.30). These data show that loss of LARP4 results in disruption of protein levels of select proteins belonging to the OXPPs and MRP gene groups that were enriched in the RNA-target sets of LARP4 from two different human cell lines.

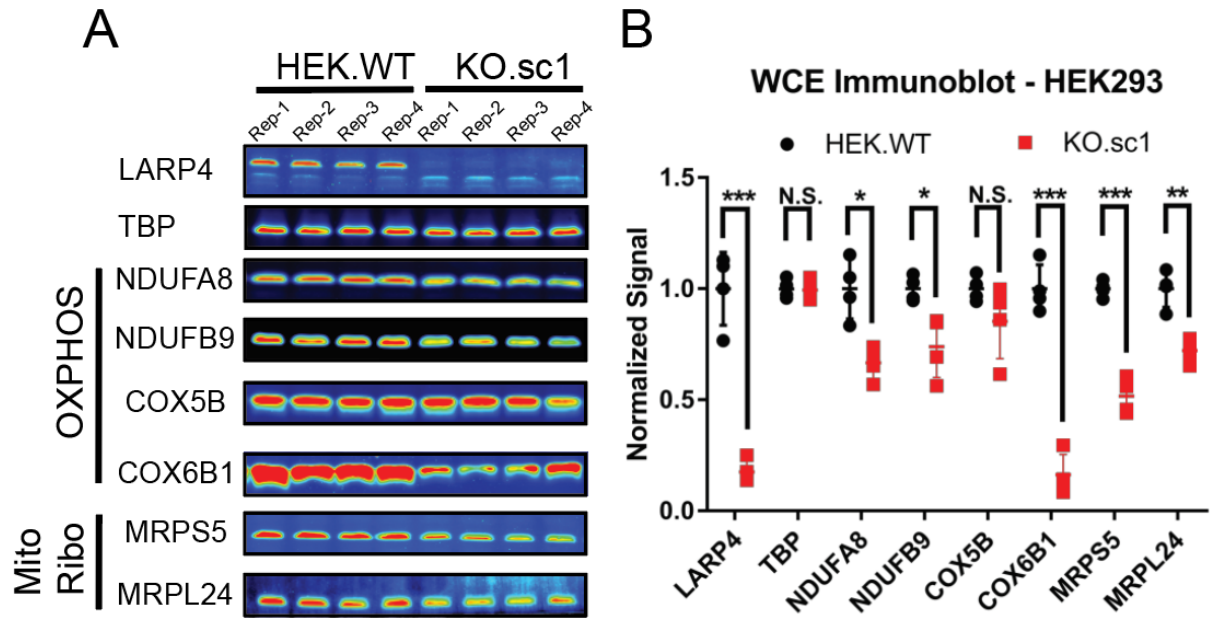


Figure 16. *Immunoblot analysis of LARP4 targets in HEK293.*
*(A)* Immunoblot analysis of various oxidative phosphorylation proteins and mitochondrial ribosome proteins in the HEK293 KO and parental WT cells. (B) Quantification of biological replicates shown in immunoblot panels. All averages shown are from independent biological replicates n=4.

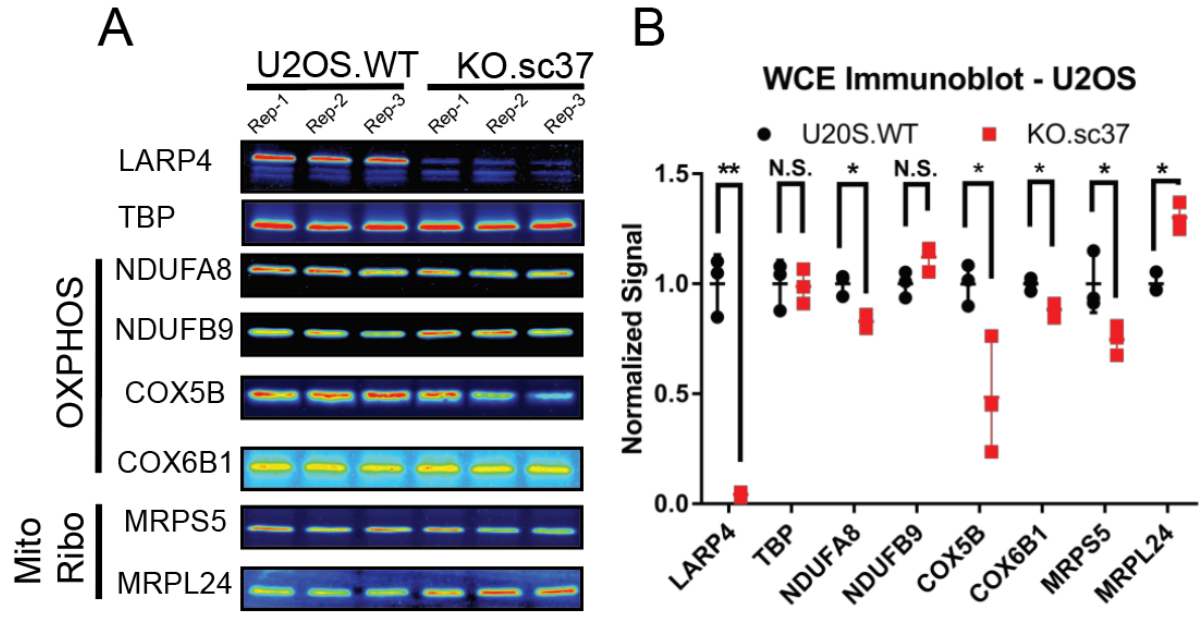


Figure 17. *Immunoblot analysis of LARP4 targets in U2OS.*
*(A)* Immunoblot analysis of various oxidative phosphorylation proteins and mitochondrial ribosome proteins in the U2OS KO and parental WT cells. (B) Quantification of biological replicates shown in immunoblot panels. All averages shown are from independent biological replicates n=3.

## 3.3 Analysis of target mRNA abundance in LARP4 knock-out HEK293 cells

Given that LARP4 is thought to stabilize the mRNA of a subset of targets in certain contexts (Mattijssen et al. 2020, Yang et al., 2011), I sought to determine if the reduction in protein levels of OXPPs and MRPs observed in the HEK293$^{LARP4-/-}$ KO cells could be explained by a corresponding reduction in abundance of their encoding mRNAs. Analysis of mRNA abundance was performed by RT-qPCR on a panel of mRNAs encoding MRPs (Figure 18A) as well as OXPPs (Figure 18B) on wild-type and HEK293$^{LARP4-/-}$ KO cells. None of the 9 mRNAs encoding MRPs tested or the 13 mRNAs encoding OXPPs tested showed a significant change in abundance relative to wild-type HEK293 cells. This indicates that the reduction in protein levels of OXPPs and MRPs observed in the HEK293$^{LARP4-/-}$ KO cells is not due to a reduction in the abundance of the encoding mRNAs. This provides support for a model in which LARP4 regulates a post-transcriptional process other than mRNA stability to promote expression of OXPPs and MRPs, such as translational efficiency or localized translation.

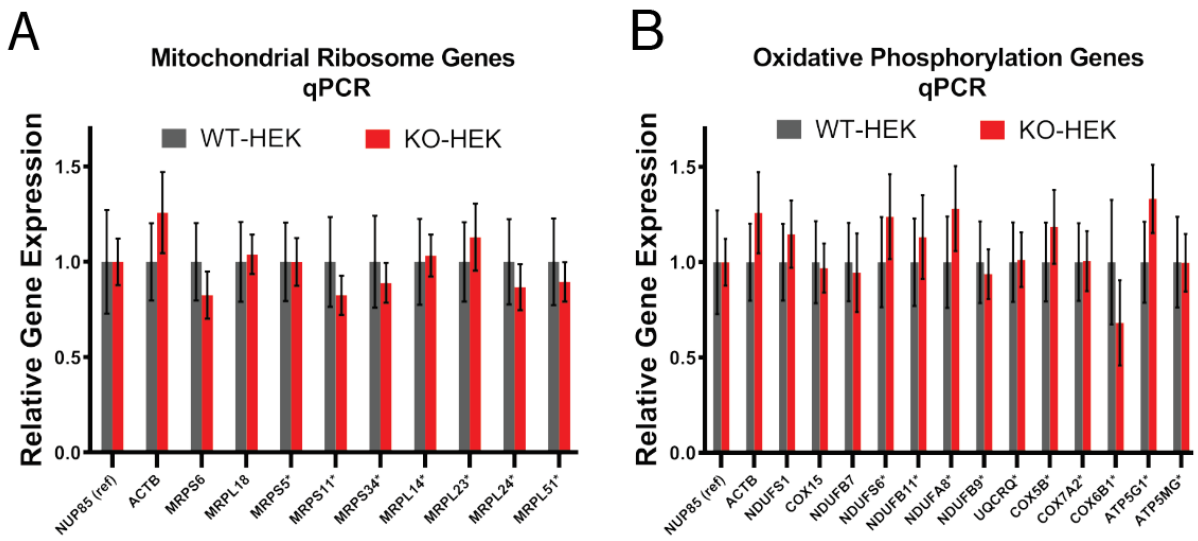


Figure 18. *Analysis of LARP4 target mRNA abundance in the HEK293 KO/WT cells by qPCR.*
Relative gene expression analysis by RT-qPCR of mRNAs encoding (A) mitochondrial ribosome proteins or (B) oxidative phosphorylation proteins. LARP4 targets are denoted with an asterisk. All averages shown are from independent biological replicates n=3.

## 3.4 Chapter 3 conclusion

In this chapter, I generate LARP4 knockout cell lines using Cas9/CRISPR gene editing in HEK293 and U2OS cell line backgrounds. Using immunoblotting, I provide evidence that loss of LARP4 disrupts protein levels of OXPP and MRP LARP4 targets. I also show through RT-qPCR analysis that loss of LARP4 does not significantly alter the mRNA levels of a panel of OXPP and MRP genes, including the LARP4 targets tested by immunoblot. Together these data show that loss of LARP4 can disrupt the protein levels without affecting the mRNA abundance of OXPP and MRP genes, suggesting that LARP4 is regulating the translation of these targets possibly by promoting localized translation in the vicinity of mitochondria.

Portions of Chapter 3 are included in a completed manuscript that has been accepted for review at Cell Reports. “LARP4 Is an RNA-Binding Protein That Binds Nuclear-Encoded Mitochondrial mRNAs To Promote Mitochondrial Function” Lewis, Benjamin; Cho, Chae Yun; Yeo, Gene; Hunter, Tony. The dissertation author was the primary investigator and author of this paper.

# Chapter 4: Quantitative proteomic analysis of LARP4 knockout cell line reveals reduced abundance of mitochondrial ribosome proteins and OXPHOS proteins.

## 4.1 Subcellular fractionation strategy and proteomic strategy

To gain more comprehensive insights into the proteomic consequences of LARP4 depletion and verify the reductions in protein abundance observed for OXPPs and MRPs by immunoblotting using an orthogonal method of measurement, quantitative tandem mass tag (TMT) proteomics was performed on HEK293$^{LARP4-/-}$ KO and wild-type cells. To gain insights into possible defects in protein localization to mitochondria in the HEK293$^{LARP4-/-}$ KO cells subcellular fractionation was performed in parallel (Figure 19). A rapid-magnetic mitochondrial enrichment strategy was used to generate two types of protein extracts for each genotype, a whole-cell extract (WCE) and a mitochondrial fraction extract (MITO) from the same cultures. Biological replicates (N=4) of each type of protein extract were processed and analyzed by separate quantitative TMT proteomic experiments, to produce a WCE-TMT dataset (Figure 20A) and a MITO-TMT dataset (Figure 20B).

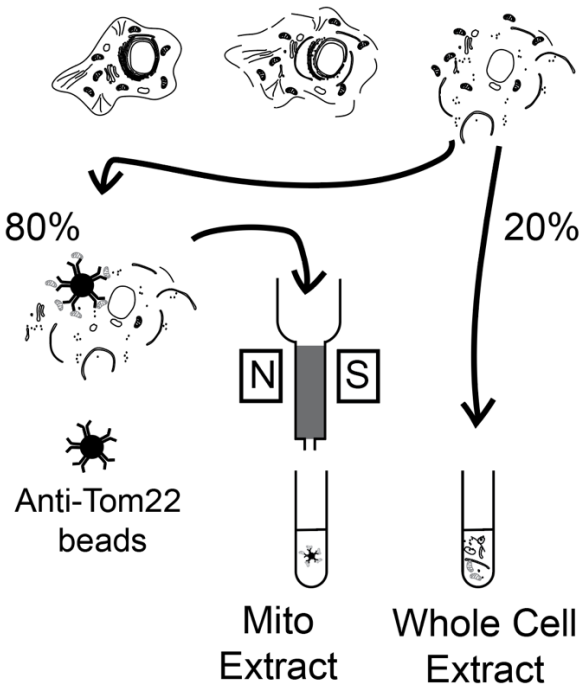


Figure 19.*Diagram of subcellular fractionation and proteomics strategy*

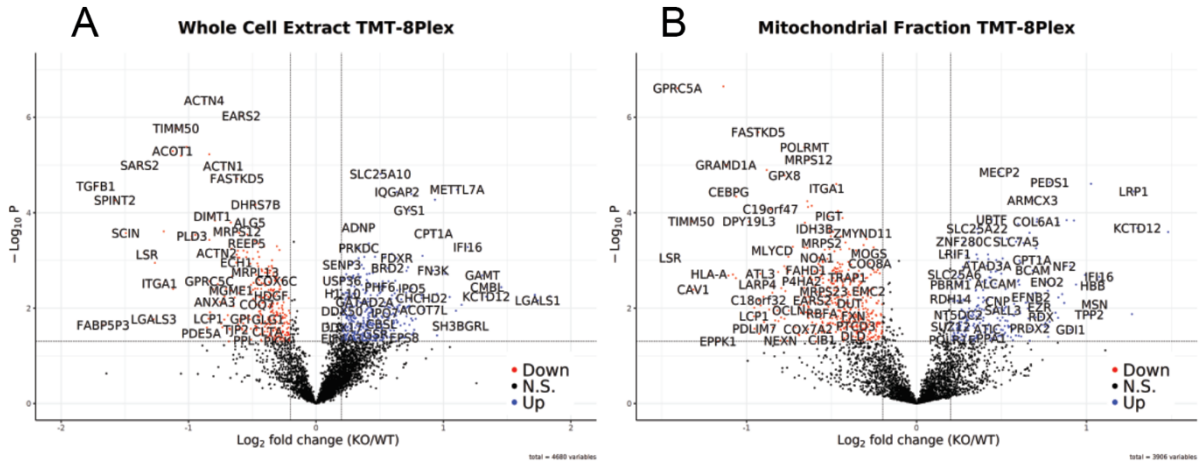


Figure 20. *Quantitative proteomic analysis of HEK293$^{LARP4-/-}$ KO cell line*.
(A) Volcano plot showing proteins abundance (tag ratio of KO/WT) results from quantitative tandem mass tagging (TMT) analysis of whole cell extracts (n=4) prepared form HEK293$^{LARP4-/-}$ KO cells and wild-type cells. (B) Volcano plot showing proteins abundance results from quantitative tandem mass tagging (TMT) analysis of mitochondrial enriched extracts (n=4).

## 4.3 Gene ontology analysis

To determine how gene groups that were overrepresented within LARP4's RNA-target set were affected by LARP4 depletion gene ontology (GO) analysis was performed on the proteomics datasets using the Metascape method (Zhou et al., 2019). For each TMT dataset (WCE or MTIO), sets of proteins present in significantly increased abundance (WCE: n=204, MITO: n=290) or decreased abundance (WCE: n=287, MITO: n=495) were defined (log2foldchange +/- 0.2 and p-value<0.05) and a separate GO analysis performed on each.

### 4.3.1 Gene ontology analysis – Proteins with decreased abundance

The GO analysis of proteins with decreased abundance in HEK293$^{LARP4-/-}$ KO cells (Figures 21A and 21B) revealed that many of the depleted proteins belonged to similar gene groups that were also overrepresented within LARP4's RNA-target set. In both proteomic datasets, two of the most enriched gene groups in the set of depleted proteins were proteins involved in mitochondrial gene expression and proteins involved in cellular respiration. In the set of depleted proteins for each dataset, the mitochondrial gene expression term (primarily composed of MRPs) had 104 (MITO) and 71 (WCE) proteins present and the cellular respiration term (almost entirely composed of OXPPs) had 60 (MITO) and 38 (WCE) proteins present (Figures 21A and 21B). These gene groups were also enriched within LARP4's RNA-target set (Figures 8A, 12B and 12C) suggesting that LARP4 binding enhances protein expression of these target mRNAs.

### 4.3.2 Gene ontology analysis – Proteins with increased abundance

Fewer proteins with significantly increased abundance in HEK293$^{LARP4-/-}$ cells were identified in both the WCE-TMT dataset (n=204) and MITO-TMT dataset (n=290). The GO analysis of these proteins with increased abundance in HEK293$^{LARP4-/-}$ cells identified gene sets involved in biological processes that could conceivably compensate for reduced cellular respiration e.g., organic anion transport (WCE-TMT and MITO-TMT), glycolysis and gluconeogenesis (WCE-TMT), and transport of small molecules (WCE-TMT and MITO-TMT) (Figures 21C and 21D). Furthermore, these biological processes were not enriched in the LARP4 RNA-target eCLIP dataset suggesting a secondary cause for their increase in protein abundance (Figure 8A). The increase in abundance of proteins with potential to compensate for reduced cellular respiration, indicate the possibility that the HEK293$^{LARP4-/-}$ KO cells have undergone some type of genetic or metabolic compensation for the loss of LARP4 and associated reduction in abundance of proteins involved in cellular respiration.

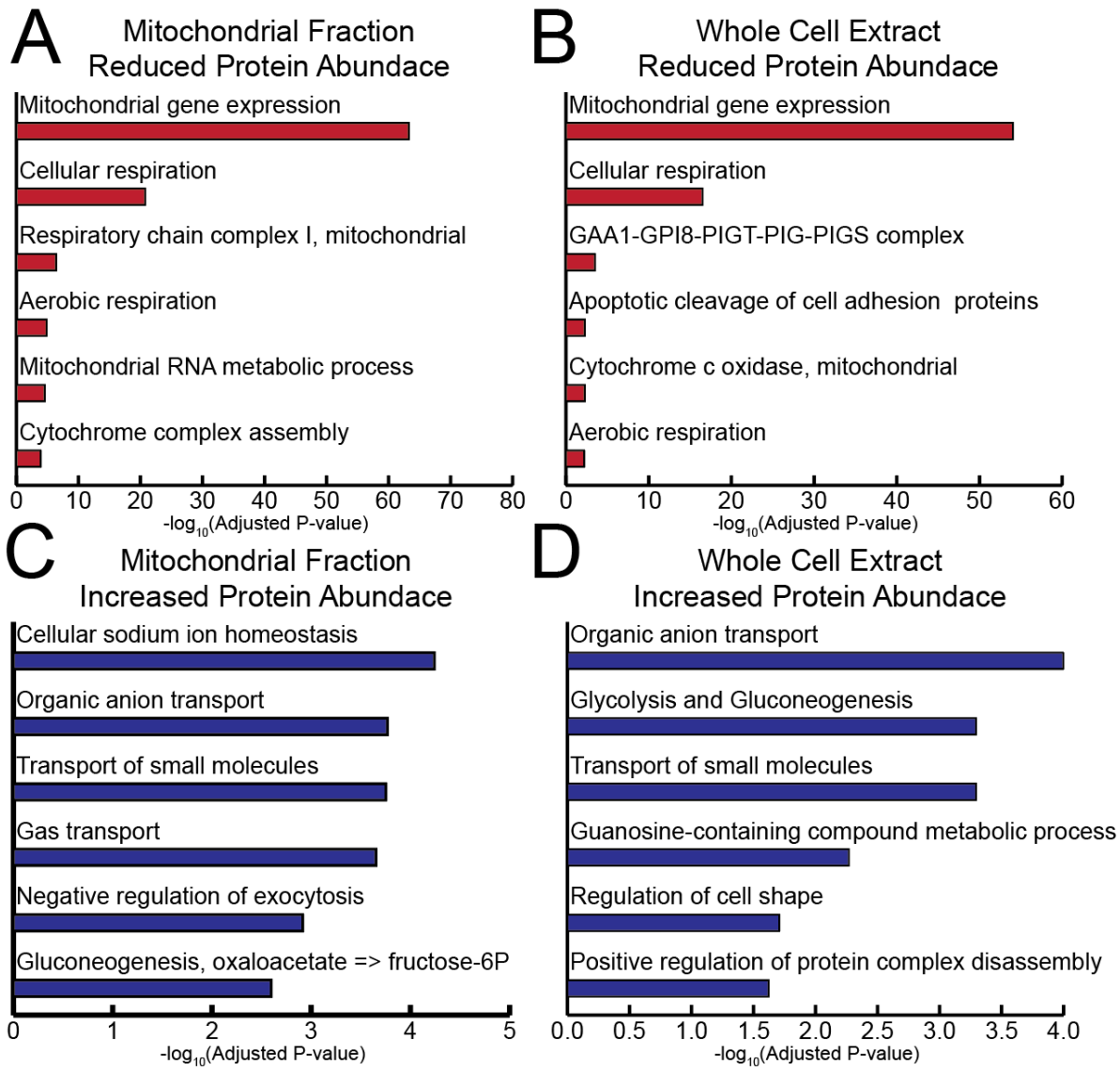


Figure 21. *Gene ontology analysis of differentially abundant proteins in HEK293 LARP4 KO cells.*
(A-B) Metascape gene ontology analysis of proteins with significant decreases in abundance identified by TMT analysis in (A) mitochondrial enriched extracts and (B) whole cell extracts. (C-D) Metascape gene ontology analysis of proteins with significant increase in abundance identified by TMT analysis in (C) mitochondrial enriched extracts and (D) whole cell extracts.

## 4.4 Mitochondrial-encoded proteins

The top gene ontology term in both proteomics datasets was mitochondrial gene expression a term primarily composed of MRPs as well as other proteins

involved in expression of the genes encoded for by the mitochondrial genome. A logical result of this would be reduced abundance of proteins expressed from the mitochondrial genome. To test this, I searched the proteomics datasets for mitochondrial-encoded proteins, and only MT-CO2 was detected. This mitochondrial-encoded protein was depleted in the HEK293$^{LARP4-/-}$ KO cells (WCE: KO/WT=0.86 and MITO:KO/WT=0.76) to levels similar to many of the nuclear-encoded OXPPs, suggesting that either the depletion of MRPs results in decreased mitochondrial translation or other biological processes such as degradation or transcriptional buffering are occurring to bring the mitochondrial-encoded and nuclear-encoded subunits of the respiratory complexes into stoichiometric balance (Taggart et al., 2020). Because mitochondrial translation was not measured, it is difficult to separate these possibilities; future studies should measure mitochondrial translation in LARP4 knockout cells.

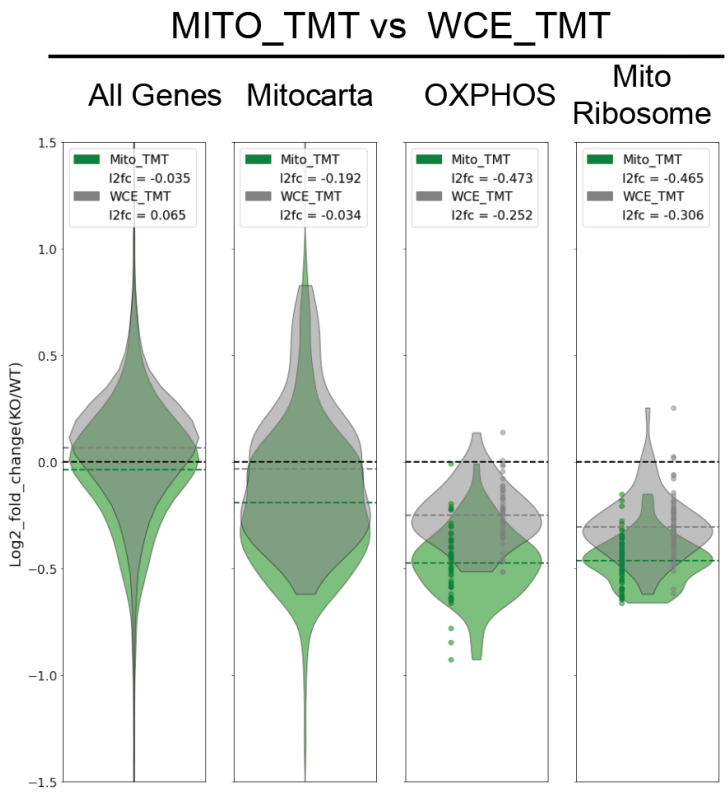


Figure 22. *Comparison of whole cell and mitochondrial extracts in HEK293$^{LARP4-/-}$ KO cells.*
Violin plots comparing the changes in protein abundance of OXPHOS proteins and mitochondrial ribosome proteins observed in the mitochondrial extract (green) and whole cell extract (grey) proteomics experiments. Distributions shown are of average (n=4) log2 fold changes (KO/WT) of each protein within each gene group with each distribution average shown as a horizontal line and displayed in the legend.

## 4.5 Comparison of WCE and MITO TMT experiments

One of the goals of creating paired mitochondrial extracts and whole cell extracts by performing subcellular fractionation in the wild-type cells and LARP4 knockout cells was to compare changes in protein abundance in the two extracts to gain insight into any possible defect in protein targeting in the LARP4 knockout cells. If LARP4 enhances protein targeting to mitochondria, then any reductions in protein abundance should be more severe in the mitochondrial extracts because less of protein will have made it into the mitochondrial fraction.

Interestingly this is what was observed when comparing the two TMT experiments; the reduction in protein abundance of OXPPs and MRPs was much more pronounced in the analysis of the mitochondrial extracts compared to the analysis of the whole cell extracts from the same cultures. For the oxidative phosphorylation proteins (OXPPs) the average fold change in protein abundance was 0.72 in the mitochondrial extracts and 0.84 in the whole cell extracts (Figure 22). A similar trend was observed for the MRPs with an average fold change of 0.73 in the mitochondrial extracts and an average fold change of 0.81 in the whole cell extracts (Figure 22), suggesting that in the HEK293$^{LARP4-/-}$ KO cells targeting of these proteins to mitochondria is impaired. These observations support a model in which LARP4 promotes both the translation and subcellular targeting of OXPPs and MRPs to mitochondria.

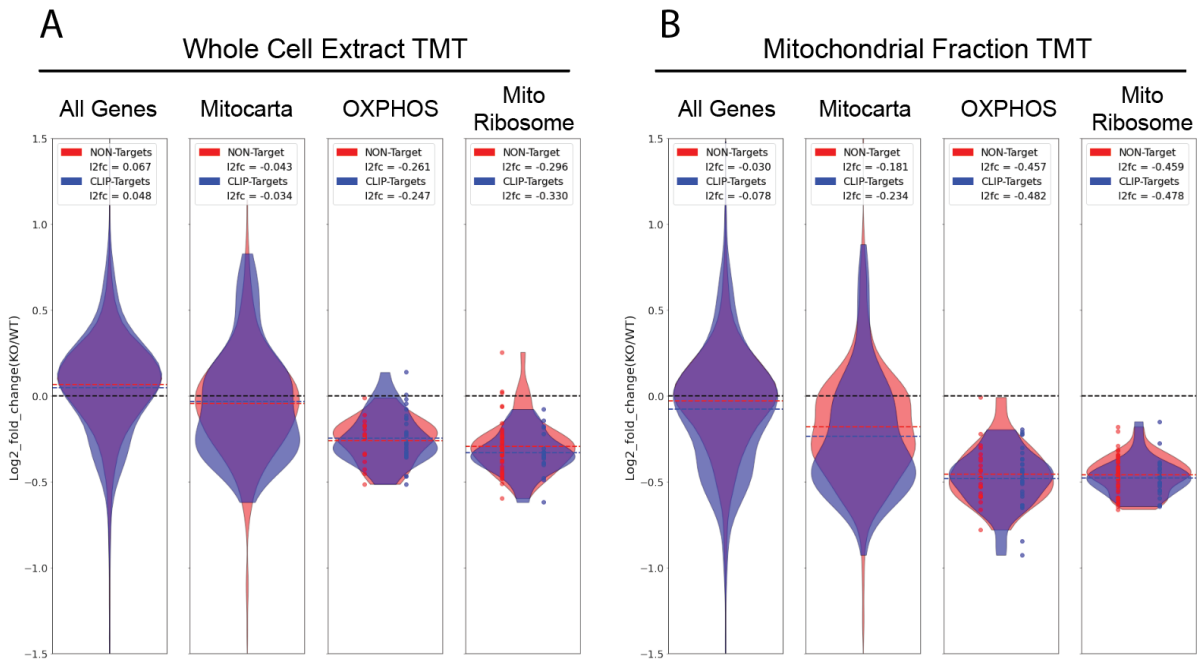


Figure 23. *Comparison of protein abundance of LAPR4 CLIP-Targets and Non-CLIP targets*.
Violin plots comparing the changes in protein abundance of LARP4 targets (blue) and non-targets (red) of various gene groups. Distributions shown are of average (n=4) log2 fold changes (KO/WT) of each protein within each gene group with each distribution average shown as a horizontal line and displayed in the legend. Analysis of the TMT-proteomics on (A) whole cell extracts and (B) mitochondrial extracts in HEK293$^{LARP4-/-}$ KO cells.

## 4.6 Comparison of eCLIP targets and non-eCLIP targets

An unresolved question is what effect does LARP4 binding have on the abundance of the proteins encode by the RNA-targets of LARP4. To gain insight into this question using the proteomics datasets, I compared the change in protein abundance following LARP4 depletion of LARP4 targets and non-targets. I also made separate comparisons within each dataset for all genes, mitochondrial genes, OXPHOS genes and MRP genes (Figures 23A and 23B). For the WCE-TMT and MITO-TMT datasets the average log2 fold change (KO/WT) in protein abundance for LARP4 targets and non-targets was very similar for the OXPHOS and MRPs

subgroups of proteins. One possible explanation for this is that the abundance of both LARP4 targets and non-targets that encode for proteins that form multi-protein complexes to change together due to the biological processes that keep the proportions of protein complex components in stoichiometric balance, such as degradation of orphan subunits (Taggart et al., 2020). This is especially relevant for the OXPHOS and MRP gene groups because they are almost entirely composed of proteins that form large multi-protein complexes (i.e., the respiratory chain complexes or the mitochondrial ribosome). Furthermore, LARP4 targets make up a large fraction of the total number of proteins in each group. Even at the more conservative threshold for a significant eCLIP peak used this comparison (l2fc>4 and -log10pvalue>7) 65% of OXPHOS proteins and 31% of MRPs detected in the MITO TMT experiment are LARP4 targets but at the less conservative baseline threshold for eCLIP targets (l2fc>3 and -log10pvalue>3) those percentages increase to 81% for OXPHOS proteins and 66% for MRPs. For the proteins annotated as mitochondrial proteins in the MITO-TMT dataset there was a more substantial difference in change of protein abundance (KO/WT) when comparing LARP4 targets and non-targets, with LARP4 targets showing a greater reduction in abundance than non-targets (Figure 23B). Because the mitochondrial sub-group is not dominated by proteins that form large complexes, there should be less pressure on the non-target group to match abundance of the depleted LARP4 target group. For the WCE-TMT and MITO-TMT datasets the average log2 fold change (KO/WT) in protein abundance for LARP4 targets and non-targets was very similar when considering all genes (Figures 23A and 23B). Together, these data indicate that how LARP4 depletion modulates the

protein abundance of RNA-targets of LARP4 is complex and likely different for non-mitochondrial RNA-targets.

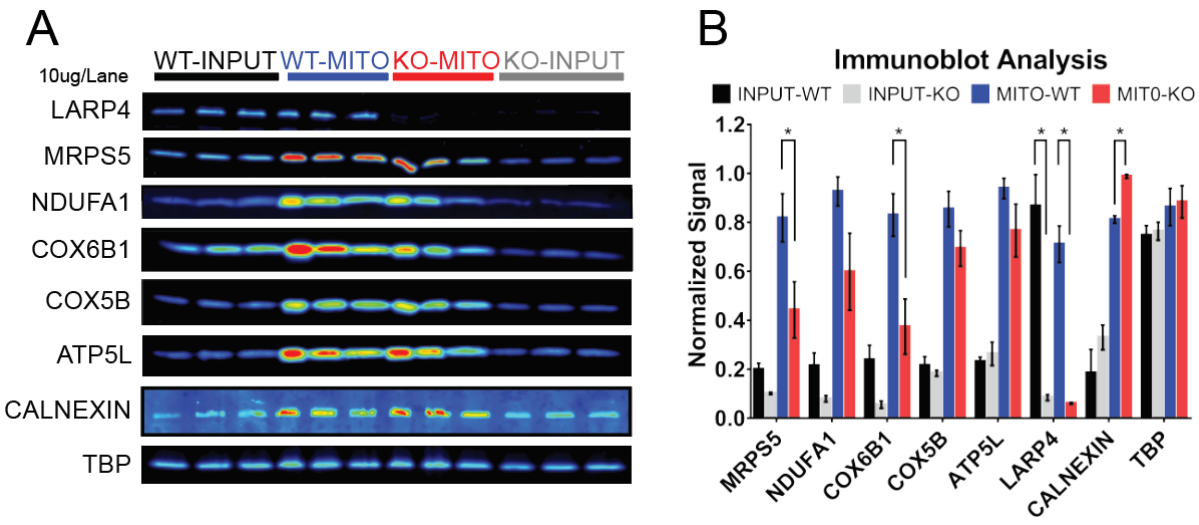


Figure 24. *Immunoblot analysis of subcellular fractionation in LARP4 KO/WT cells.* (A) Immunoblot analysis of whole cell extracts (input) and mitochondrial enriched extracts, from each lane was load with 10 ug of protein.(B) Quantification of immunoblot analysis. All averages shown are from independent biological replicates n=3. Significant difference resulting in a p value of < 0.05 are denoted with an * symbol (paired students t-test).

## 4.7 Immunoblot validation

To validate some of the changes in protein abundance observed in the TMT experiments, quantification of protein abundance by immunoblot analysis of selected OXPPs and MRPs was also performed on similar WCE extracts and MITO extracts produced while optimizing the mitochondrial enrichment strategy. Although increased variability in these pilot experiments reduced the significance of some comparisons significant differences were observed (MRPS5 and COX6B1) as well downward trends similar to observations from the proteomics data (Figures 24A and 24B).

## 4.8 Chapter 4 conclusion

In this chapter, I use subcellular fractionation and quantitative TMT proteomics to analyze changes in protein abundance in whole cell extracts and mitochondrial extracts from LARP4 knockout cells. This analysis indicates that the gene groups that were overrepresented in the set of proteins depleted in LARP4 knockout cells, were very similar to the gene groups overrepresented in the RNA-target sets of LARP4. Genes involved in oxidative phosphorylation (i.e., OXPPs) and mitochondrial gene expression (i.e., MRPs) were the most overrepresented in gene groups in the set of depleted proteins from each of the proteomics datasets. It was also noteworthy that the depletion of OXPPs and MRPs was more severe in the mitochondrial extracts, suggesting a deficit in protein targeting to mitochondria in the LARP4 knockout cells. Together these data provide support for a model in which LARP4 binding to OXPPs and MRPs transcripts supports their translation and subcellular targeting to mitochondria.

Portions of Chapter 4 are included in a completed manuscript that has been accepted for review at Cell Reports. “LARP4 Is an RNA-Binding Protein That Binds Nuclear-Encoded Mitochondrial mRNAs To Promote Mitochondrial Function” Lewis, Benjamin; Cho, Chae Yun; Yeo, Gene; Hunter, Tony. The dissertation author was the primary investigator and author of this paper.

## Chapter 5: Loss of LARP4 reduces cell proliferation rates, levels of oxidized proteins, translational rates and oxidative phosphorylation function.

After identifying the functionally related RNA-targets of LARP4 and demonstrating that key mitochondrial proteins were depleted in LARP4 knockout cells, I wanted to understand if there are related functional consequences due to the loss of LARP4. To address this question several cellular and mitochondrial specific functional phenotypes were assayed. For cellular phenotypes proliferation rates were measured in both HEK293 and U2OS LARP4 knockout cells as well as translation rates in HEK293 knockout cells. Several mitochondrial specific functional phenotypes were also assayed in HEK293 knockout cells including, levels of oxidized proteins, oxygen consumption rates and mitochondrial membrane potential.

### 5.1 Proliferation rates are reduced in LARP4 knockout cells

Given the essential role of mitochondria in cell proliferation (Birsoy et al., 2015; Sullivan at al., 2015) and the depletion of proteins essential to mitochondrial function in observed in LARP4 knockout cells, I hypothesized that cell proliferation would be reduced in LARP4 knockout cells. Cell proliferation studies showed that the HEK293$^{LARP4-/-}$ knockout cells had significantly reduced proliferation rates; averages from independent experiments (N=3) showed significantly increased cell doubling times relative to wild-type cells, and this reduction in the rate of cell proliferation was completely rescued by re-expression of full length LARP4 (isoform A) (Figure 25A). A reduced rate of cell proliferation was also observed in the U2OS$^{LARP4-/-}$ knockout cells compared to wild-type cells in two independent experiments (Figure 25B). These data indicate that LARP4 is required for normal rates of proliferation in HEK293 cells

and LARP4 depletion is also associated with reduced proliferation rates in the U2OS cancer cell line.

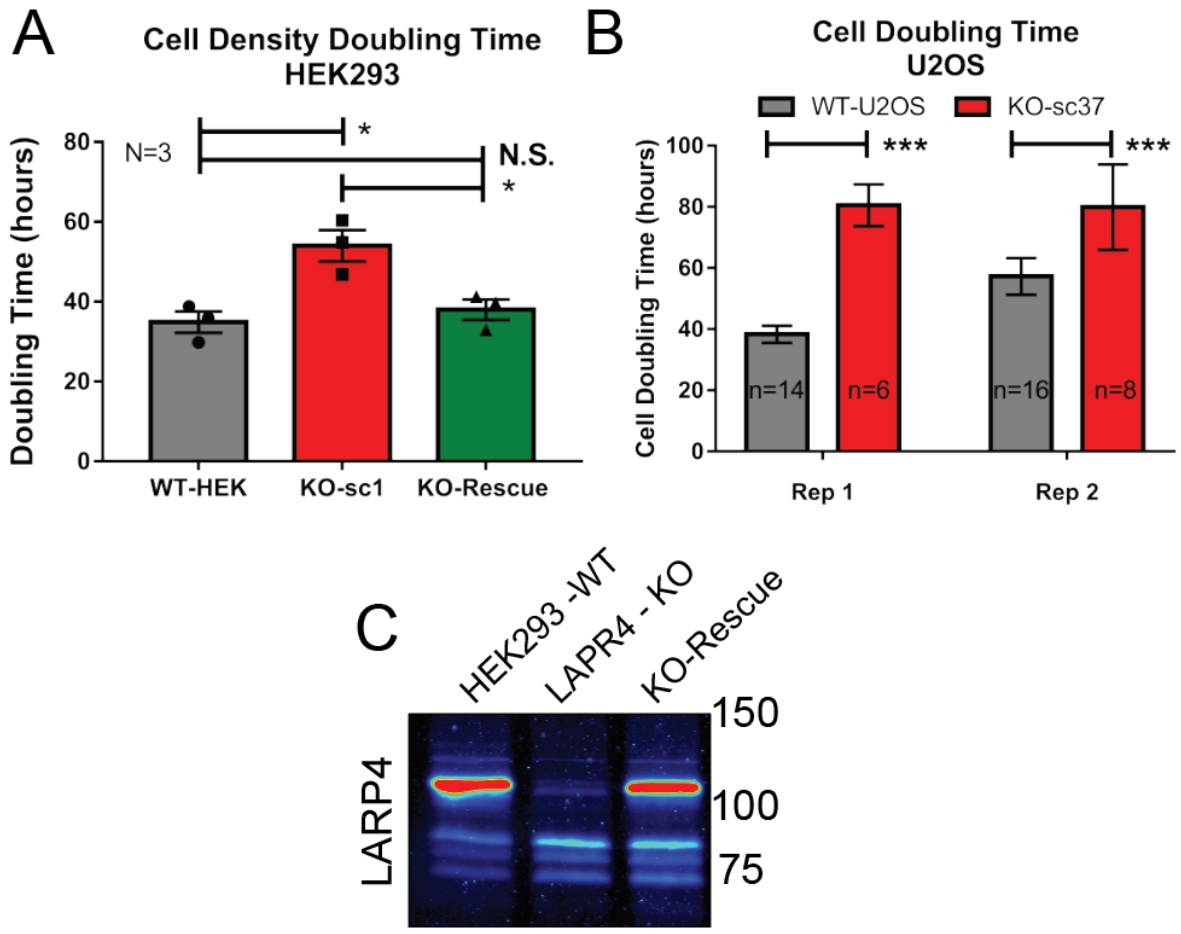


Figure 25. *Loss of LARP4 reduces cell proliferation rates.*
(A) A summary plot of average confluency doubling times for wild-type HEK293 cells, HEK293$^{LARP4-/-}$ KO cells and HEK293$^{LARP4-/-}$ KO-Rescue cells from independent experiments (N=3). (B) A plot of cell doubling times of wild-type U2OS cells and U2OS$^{LARP4-/-}$ KO cells, averages of technical replicates from each of two independent experiments are shown (Rep 1 and Rep 2). (C) An immunoblot showing expression of LARP4 in the HEK293$^{LARP4-/-}$ KO-Rescue cells.

## 5.2 LAPR4 is required for normal translation rates

LARP4 has been shown to associate with translational machinery (Yang et al., 2011) and to enrich mRNAs encoding translational proteins in its RNA-target set (Figures 8A, 8B and 9B). Additionally, protein translation is energy intensive and

LARP4 targets and regulates expression of proteins essential to the energy producing capacity of mitochondria. For these reasons I wanted to assay translation rates, and for this purpose used the puromycin incorporation assay. The translation rates in the HEK293$^{LARP4-/-}$ knockout cells were found to be substantially reduced relative to the wild-type cells as measured by the normalized puromycin incorporation signal. Additionally, re-expression of LARP4 returned translation rates to levels similar to levels in wild-type cells (Figures 26A-26D). These data indicate that LARP4 is required for normal translation rates in HEK293 cells. Translational proteins were one of gene groups enriched in the RNA-target of LARP4; however, in mass spectrometry data, the protein levels of cytosolic translation proteins were not significantly affected by loss of LARP4. This suggests that LARP4 either directly promotes protein global translation rates through its own interactions or indirectly through promoting mitochondrial function to provide energy to sustain the energy intensive process of translation.

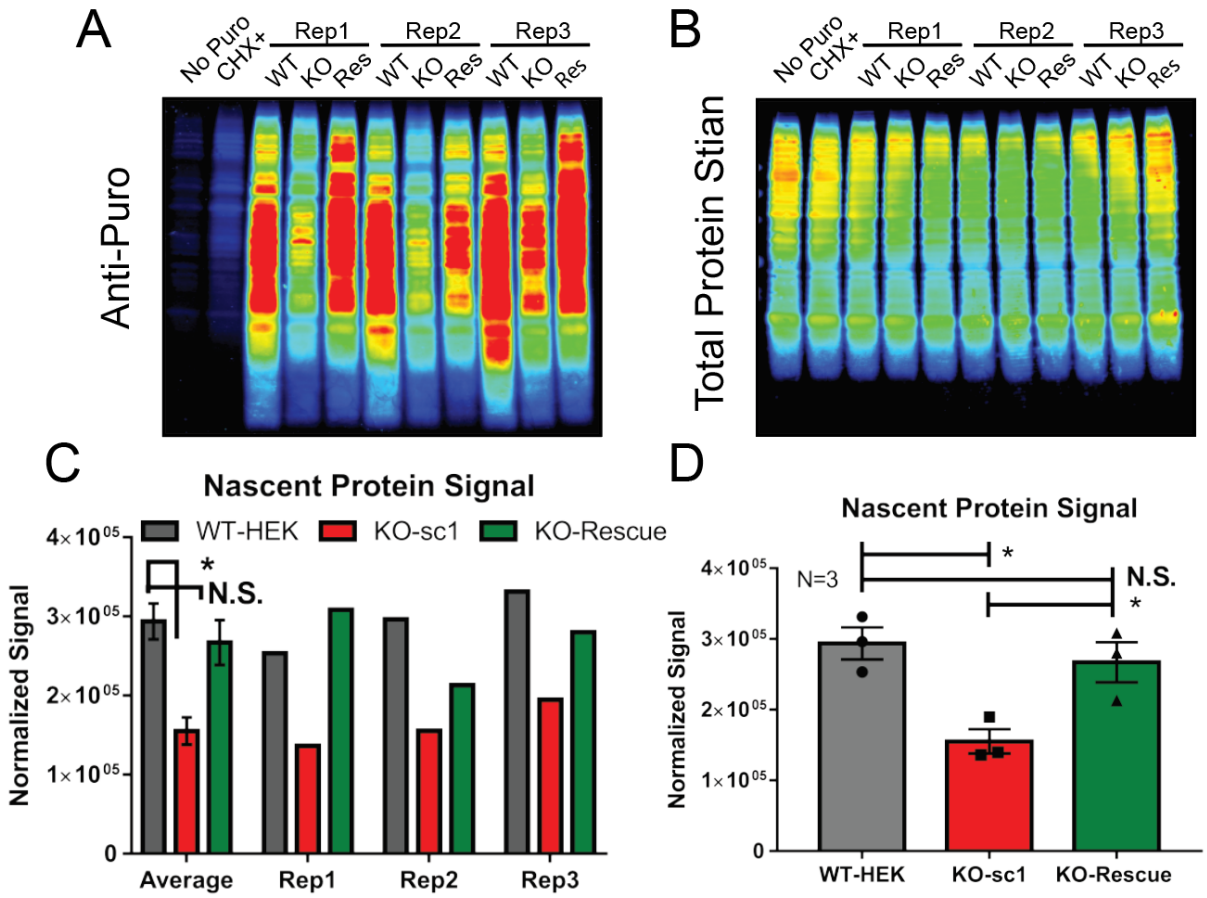


Figure 26. *Loss of LARP4 reduces protein translation rates.*
(A) An anti-Puromycin immunoblot probing for the nascent proteins terminated by puromycin. (B) A quantitative total protein stain of the blot in panel A used for normalization. (C) A bar graph showing the normalized puromycin incorporation signal for each of the replicates. (D) A summary plot of average (N=3) normalized puromycin incorporation signal from biological replicates.

## 5.3 Oxidized protein levels are reduced in LARP4 knockout cells

Because mitochondria are a major source of reactive oxygen species (Balaban et al., 2005), which are a cause of protein oxidation, and many OXPHOS related proteins are depleted in the LARP4 knockout cells, I hypothesized that protein oxidation would be reduced in the LARP4 knockout cells. For these reasons, levels of oxidized proteins were measured, using a derivatization and immunoblot approach

(Oxiblot Kit). This analysis found that oxidized proteins were present in significantly lower abundance in HEK293$^{LARP4-/-}$ knockout cells compared to wild-type cells, and that this phenotype was completely rescued by re-expression of LARP4 (Figures 27A-27D). These data indicate that LARP4 promotes the production of oxidized proteins, likely through promoting mitochondrial respiration rates.

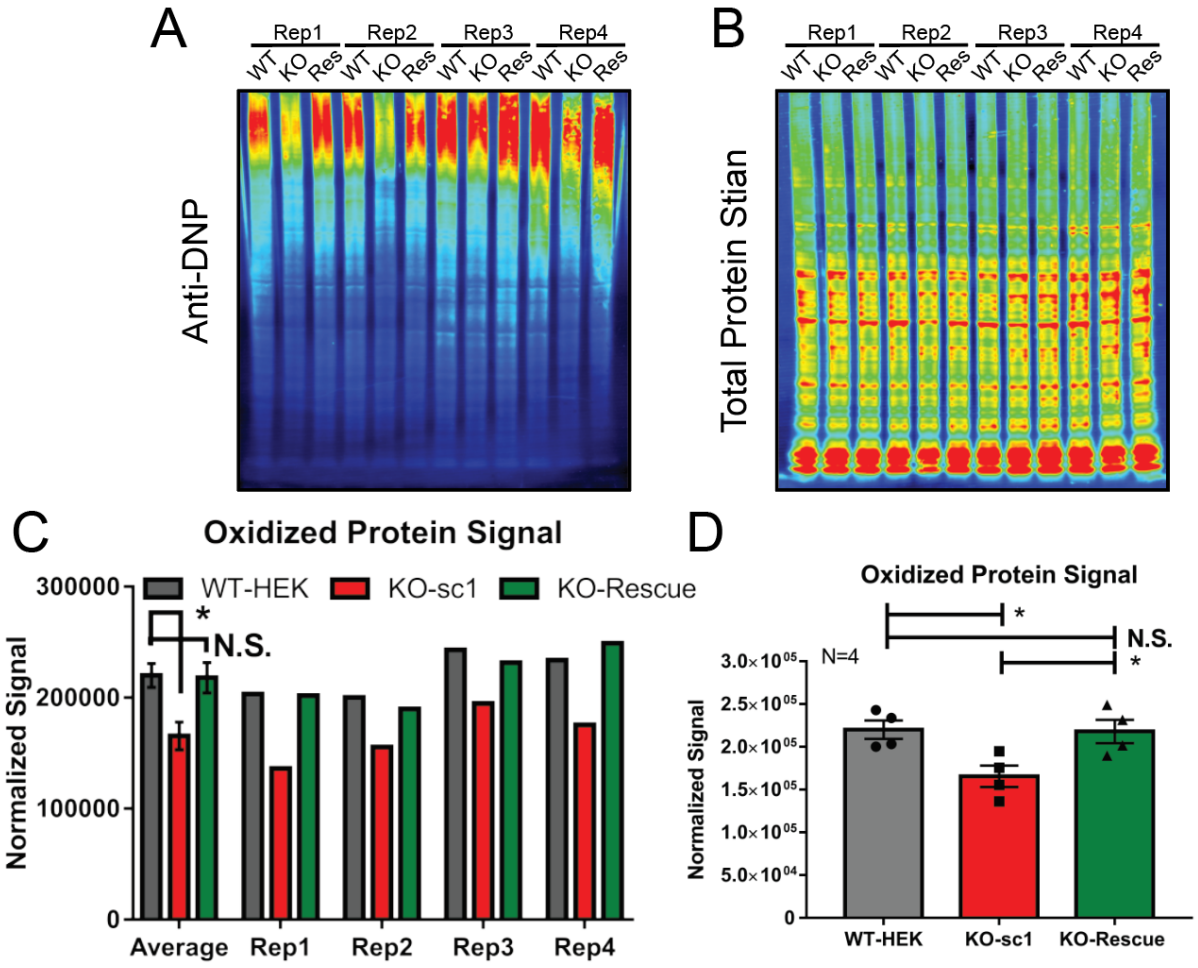


Figure 27. *Loss of LARP4 reduces levels of oxidized proteins.*
(A) An anti-DNP immunoblot probing for the derivatized oxidized proteins. (B) A quantitative total protein stain of the blot in panel A used for normalization. (C) A bar graph showing the normalized oxidized protein signal for each of the replicates. (D) A summary plot of average (n=4) normalized oxidized protein signal from biological replicates.

## 5.4 LARP4 promotes oxidative phosphorylation function

As proteins essential for cellular respiration (OXPPs and MRPs) were significantly depleted in the HEK293$^{LARP4-/-}$ knockout cells, the functional impact on oxidative phosphorylation (OXPHOS) function and capacity was investigated. The Seahorse Extracellular Flux Analyzer was used to measure oxygen consumption rates (a parameter directly related to OXPHOS function). The analyzer was configured to run the Mito-stress-test assay which assesses basal respiration and maximal respiration, measured in terms of oxygen consumption rates (OCR).

In every Mito-stress-test Seahorse assay performed, the HEK293$^{LARP4-/-}$ knockout cells exhibited significantly reduced basal respiration and maximal respiration compared to wild-type cells (Figures 28A-28F). Similarly, the U2OS$^{LARP4-/-}$ knockout cells exhibited deficiencies in OXPHOS function as measured by the Mito-stress-test Seahorse assay (Figures 29A-29F). Furthermore, I demonstrate that rescue of LARP4 depletion by overexpression of LARP4 in HEK293$^{LARP4-/-}$ knockout cells significantly improved the OXPHOS deficiency in the LARP4 deficient cells although not completely to wild-type levels (Figures 28A-28F). It is likely that the LARP4 knockout cells undergo compensatory metabolic changes following genetic disruption of LARP4 and these changes prevent a complete restoration of OXPHOS rates upon LARP4 reexpression. Evidence of compensatory metabolic change were observed in the analysis of the HEK293$^{LARP4-/-}$ knockout cells by TMT-proteomics e.g., upregulation of proteins involved in glycolysis and gluconeogenesis (Figures 21C and 21D). These results from two different human cell lines demonstrate that loss of LARP4 reduces oxidative phosphorylation rates, indicating that depletion of

OXPPs and MRPs observed in LARP4 knockout cells by TMT-proteomics and immunoblot analysis has a functional impact on the biological processes carried out by these protein complexes.

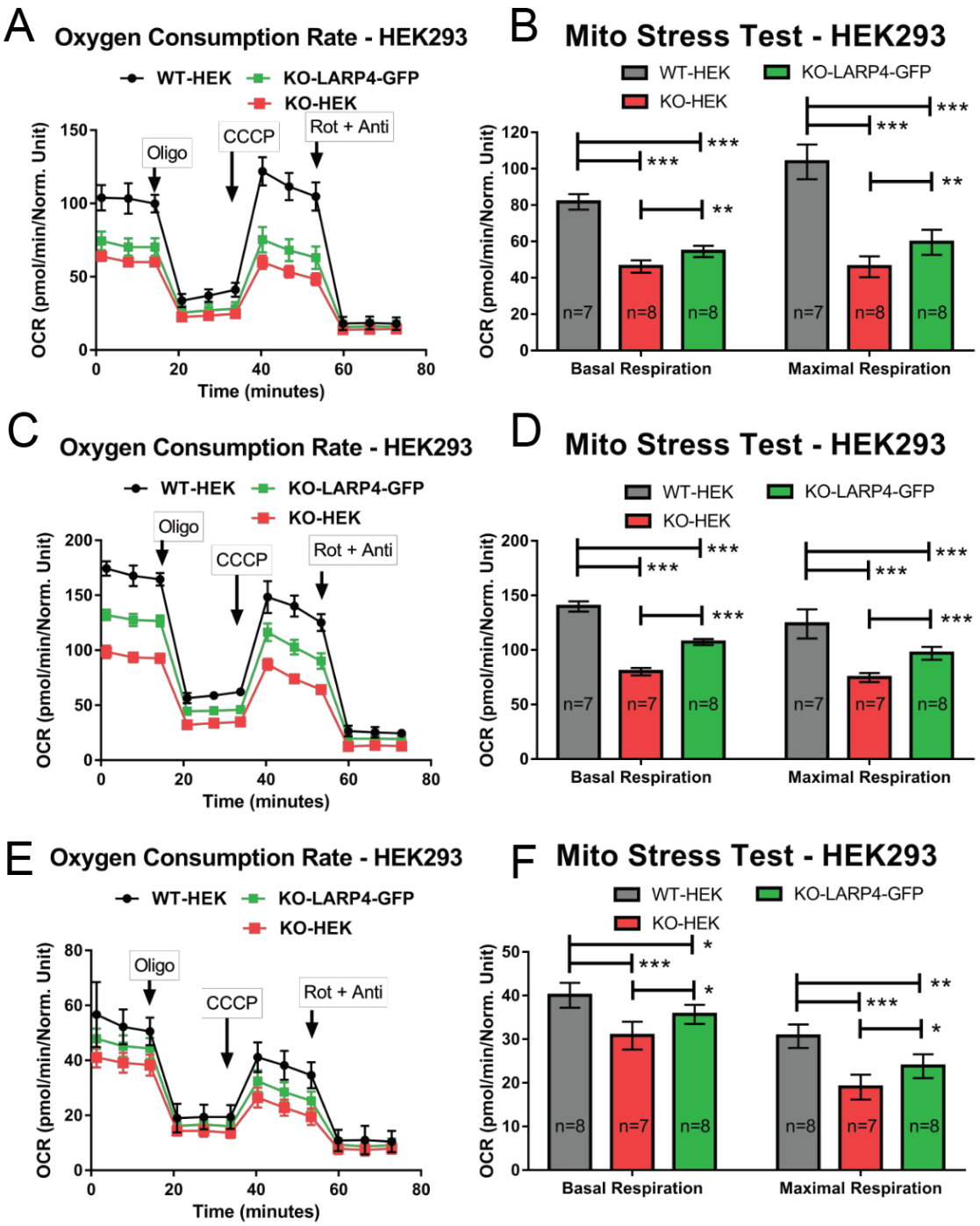


Figure 28. *LARP4 promotes oxidative phosphorylation function in HEK293 cells.* Seahorse extracellular flux analysis of oxygen consumption rates (OCR) during the mito-stress test from wild-type HEK293 cells, HEK293$^{LARP4-/-}$ KO cells and HEK293$^{LARP4-/-}$ KO-LARP4-GFP Rescue cells. Basal and maximal respiration rates are calculated from the changes in OCR in response to inhibitor addition. (A-B) Biological replicate 1. (C-D) Biological replicate 2. (E-F) Biological replicate 3.

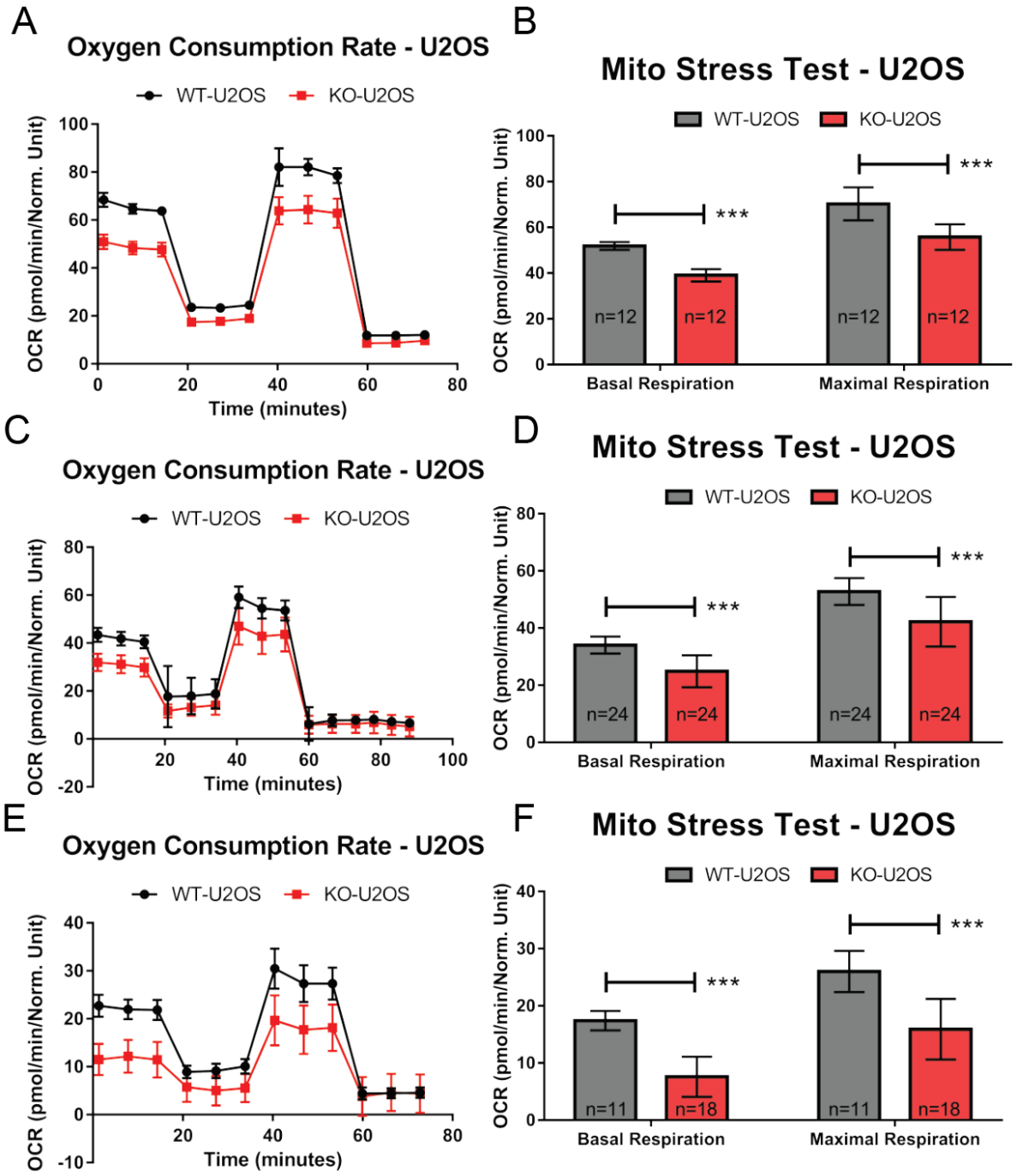


Figure 29. *LARP4 depletion reduces oxidative phosphorylation function in U2OS cells.*

Seahorse extracellular flux analysis of oxygen consumption rates (OCR) during the mito-stress test from wild-type U2OS cells and U2OS $^{LARP4-/-}$ KO cells. Basal and maximal respiration rates are calculated from the changes in OCR in response to inhibitor addition. (A-B) Biological replicate 1. (C-D) Biological replicate 2. (E-F) Biological replicate 3.

## 5.5 Mitochondrial membrane potential disruption

The effect of reduced OXPHOS rates on the mitochondrial membrane potential (MMP) was also explored in LARP4 deficient cells. Flow cytometry analysis on the HEK293$^{LARP4-/-}$ knockout cells stained with both TMRM (MMP dependent) and Mitotracker green (Mitochondrial mass dependent, MMP independent) showed a significantly reduced MMP as measured by the ratio of TMRM staining and Mitotracker green staining (Figures 30A, 30B and 30C). The MitoTracker green staining showed no significant difference between HEK293$^{LARP4-/-}$ knockout cells and wild-type cells (Figure 30C). Analysis of mtDNA levels was also performed as a measure of mitochondrial mass. This analysis found no significant difference in mtDNA levels between the HEK293$^{LARP4-/-}$ knockout cells and wild-type cells (Figure 30D). Indicating that significant changes in mitochondrial mass in HEK293$^{LARP4-/-}$ knockout cells is unlikely. From these data I can conclude the mitochondrial membrane potential is reduced in the HEK293$^{LARP4-/-}$ knockout cells.

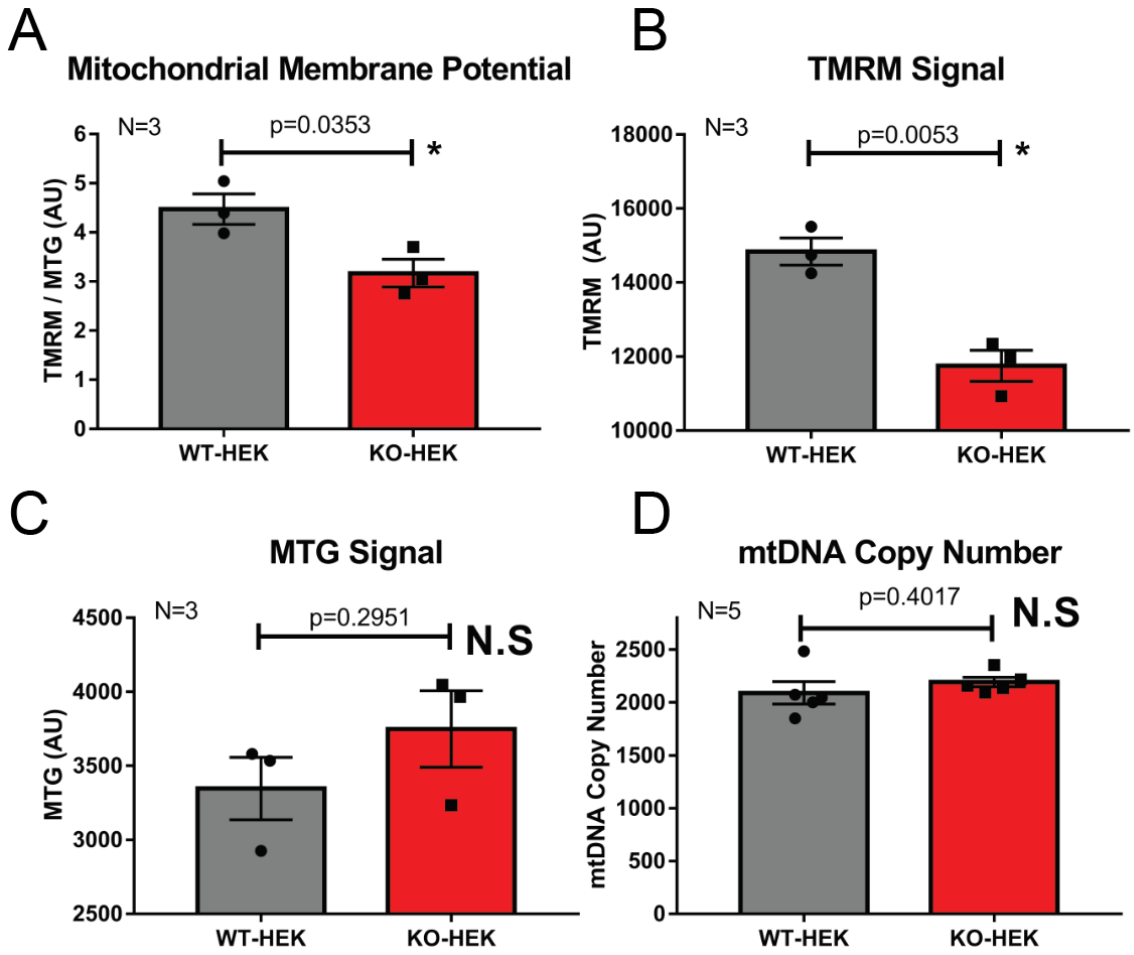


Figure 30. *LARP4 depletion reduces mitochondrial membrane potential in HEK293$^{LARP4-/-}$ KO cells.*
Analysis of mitochondrial membrane potential by flow cytometry of wild-type HEK293 cells and HEK293$^{LARP4-/-}$ KO cells stained with the potential dependent dye TMRM and the potential independent dye MitoTracker Green. Averages shown are from three independent experiments (N=3). (A) Average TMRM signal normalized by MTG signal. (B) Average signal per cell from the TMRM dye without normalization. (C) Average signal per cell from the MTG dye. (D) Analysis mitochondrial mass by proxy using qPCR measurements of mitochondrial DNA copy number from wild-type HEK293 cells and HEK293$^{LARP4-/-}$ KO cells samples. Averages shown are from samples from five independent experiments (N=5).

## 5.6 Chapter 5 conclusion

In previous chapters, I established that some of the most prominent gene groups in the RNA-target set of LARP4 are genes involved in oxidative phosphorylation (OXPPs) and mitochondrial translation (MRPs) and protein levels of

both OXPPs and MRPs are depleted upon loss LARP4. In this chapter, I provide evidence that the depletion of these proteins essential for oxidative phosphorylation (i.e., OXPPs and MRPs) observed in the LARP4 knockout cells has functional consequences oxidative phosphorylation as well as other processes that oxidative phosphorylation promotes. Cellular proliferation, which requires a functioning OXPHOS pathway, was significantly reduced in LAPR4 knockout cells and restored to normal levels following re-expression of LARP4. Protein translation, which is energy intensive, was also significantly reduced in LAPR4 knockout cells and restored to normal levels following re-expression of LARP4. Oxidative phosphorylation was also measured directly and shown to be reduced in the LARP4 knockout cells and partially restored upon re-expression of LARP4. Based on the multiple rescue experiments significant CRISPR off-targets are unlikely to have occurred. Additionally, processes promoted by OXPHOS function, such as mitochondrial membrane potential and levels oxidized proteins were reduced in LARP4 knockout cells. Together these data demonstrated that loss of LARP4 has significant functional consequences on oxidative phosphorylation and associated processes.

Portions of Chapter 5 are included in a completed manuscript that has been accepted for review at Cell Reports. “LARP4 Is an RNA-Binding Protein That Binds Nuclear-Encoded Mitochondrial mRNAs To Promote Mitochondrial Function” Lewis, Benjamin; Cho, Chae Yun; Yeo, Gene; Hunter, Tony. The dissertation author was the primary investigator and author of this paper.

# Chapter 6: Discussion and future directions

## 6.1 Discussion

The expression of mitochondrial proteins presents several unique biological challenges that must be overcome to ensure mitochondrial protein homeostasis and function. The overwhelming majority of mitochondrial proteins are encoded by mRNAs transcribed from nuclear genes, all of which must be translated by cytosolic ribosomes and imported into mitochondria by various partially redundant pathways (Bykov et al., 2020). These pathways include polypeptide dependent pathways, facilitated by the N-terminal mitochondrial targeting sequence present on many but not all mitochondrial proteins (Bolender et al., 2008), as well as mRNA dependent targeting pathways, which are facilitated by RNA-binding proteins (RBPs) that influence the abundance, spatial distribution, and translational activity of their RNA-targets (Bethune et al., 2019).

Efficient targeting of proteins to mitochondria is particularly important for certain classes of proteins. These include proteins whose ectopic expression in the cytosol has potentially deleterious effects for the cell. This has been demonstrated for both oxidative phosphorylation proteins (OXPPs) and mitochondrial ribosome proteins (MRPs) (Boos et al., 2019; Bykov et al., 2020; Rawat et al., 2019; Williams et al., 2014; Wrobel et al., 2015; Yoo et al., 2005). Additionally, for proteins that assemble into large multi-protein complexes, such as OXPPs and MRPs (Figure 2A), spatial and temporal coordination of translation also has the potential to promote co-translational complex assembly, a process that has been demonstrated to be

beneficial in several contexts (Kamenova et al., 2019; Keil et al., 2012; Schwarz et al., 2019).

Post-transcriptional regulation of nuclear-encoded mitochondrial mRNAs (NEMmRNAs) including localization to mitochondrial membrane and localized translation is a fundamentally conserved biological process from yeast to metazoans; however, the protein factors (RBPs) and the mRNA sequences involved differ. A more complete characterization of the RBPs and their RNA interactions involved in this process in the context of human cells will facilitate greater insight into the mechanisms by which these RBPs promote efficient expression of mitochondrial proteins, potentially leading to a better understanding of the plethora of diseases where mitochondrial dysfunction is present.

In this report I elucidate a novel function of LARP4 by which it specifically binds select groups of functionally important NEMmRNAs to help maintain mitochondrial protein homeostasis and facilitate proper oxidative phosphorylation function. My results provide direct evidence that LARP4 binds mRNAs encoding OXPPs and MRPs and implicate LARP4 in positively regulating the expression of these proteins. Additionally, I demonstrate that LARP4 is required for normal oxidative phosphorylation rates.

In this study I found that the RNA-binding protein LARP4 is required for normal translation rates, consistent with previous reports linking LARP4 to polysome stability (Yang et al., 2011). Later studies demonstrated LAPP4 to have a functional role in maintaining poly-A tail (PAT) length across the transcriptome via competition with deadenylases (Mattijssen et al., 2017; Mattijssen et al., 2020). Interestingly, LARP4-

mediated PAT length maintenance was observed across the transcriptome, except for the subset of NEMmRNAs where LARP4 did not appear to play a significant role in maintaining PAT length (Mattijssen et al., 2020). A possible explanation for this, made possible by my results, is a model in which direct RNA-targets of LARP4, such as NEMmRNAs, are bound by LARP4 in way that does not reduce deadenylase activity, whereas indirect LARP4 RNA-targets interact with LARP4 in a way that leads to reduced deadenylase activity, possibly through competing with deadenylases for protein-protein interactions with PABPs.

Another recent study described the recruitment of LARP4 along with PABPC1 and PABC4, two of the poly-A binding protein paralogs, to the surface of mitochondria by the protein kinase A adaptor protein AKAP1 to facilitate local translation of AKAP1 associated mRNAs (Gabrovsek et al., 2020). My results are consistent with and extend beyond this study by showing that LARP4 functions not only as a general translation factor but as an RBP with a preference for mitochondrial mRNAs whose depletion results in reduced mitochondrial function. In their proteomic screen for AKAP1 interacting partners, Gabrovsek et al., 2020 also found PABC4 as a highly enriched AKAP1 interactor. Interestingly, in my analysis of the ENCODE eCLIP datasets I found that PABC4 also has an RNA-target set highly enriched for NEMmRNAs. Future studies should investigate what role PABC4 plays in the expression of NEMmRNAs and if AKAP1, LARP4 and PABC4 function cooperatively.

The data presented in this study suggest that post-transcriptional processes maintained by LARP4 are responsible for the reduced abundance of certain proteins encoded for by LARP4 target mRNAs, such as OXPPs or MRPs. However, in this

study I do not provide direct evidence of which post-transcriptional processes drive the changes in gene expression observed in LARP4 depleted cells. Because I did not observe significant changes in mRNA abundance in the LARP4 target genes studied, it is unlikely that LARP4 functions a selective regulator of transcript stability in the context of OXPPs or MRPs. Given that recruitment of LARP4 to the cytoplasmic surface of mitochondria has been demonstrated (Gabrovsek et al., 2020), LARP4 may play a direct role in the recruitment of a subset of its target mRNAs, such as NEMmRNAs, to the vicinity of mitochondria to enhance local translation and mitochondrial protein targeting. Additionally, in my proteomic analysis I found that the reduction in protein abundance of OXPPs and MRPs in LARP4 knockout cells was much more pronounced in analysis of mitochondrial extracts compared to similar analysis of whole cell extracts, consistent with LARP4 playing a role in enhancing protein targeting to mitochondria.

## 6.2 Unresolved questions and future directions

This work has elucidated a novel role of LARP4 as an RBP that functions in maintaining mitochondrial protein homeostasis and OXPHOS function in doing so provokes additional questions that remain unanswered providing the justification for additional studies. The two most prominent unresolved questions are, how does LARP4 enhance the expression of OXPPs and MRPs and how does LARP achieve its RNA-target specificity?

The data supporting an enrichment of mRNAs encoding OXPPs and MRPs in the RNA-target set of LARP4 is strong and robust, and so are the data showing that LARP4 depletion results in reduced steady state levels of these proteins, without a

corresponding change in mRNA abundance. What is unclear is, how does LARP4 binding to these mRNAs enhance the abundance of these proteins? The totality of the evidence supports model in which LARP4 promotes localized translation and protein targeting of OXPPs and MRPs. I proposed three possible mechanisms that could facilitate this model: (1) LARP4 positively influences the localization of the mRNAs to vicinity of mitochondria resulting in a higher percentage of transcripts translated near mitochondria, (2) LARP4 promotes localized translation by translational activation of target mRNAs once they reach mitochondria, (3) LARP4 acts through reversible translational repression of target mRNAs away from mitochondria to promote localized translation. These mechanisms are not mutually exclusive and could contribute to protein targeting of LARP4 targets varying degrees depending on the context.

Future studies should design experiments to test these possibilities. Currently there are not robust methods available to directly measure the relative amount of local translation occurring near mitochondria in mammalian cells. Only in yeast has this been made possible using proximity-label of mitochondria (Williams et al., 2014). Because of this, future studies should focus on testing if LARP4 depletion results in reduced mitochondrial localization of LARP4's mitochondrial mRNA-targets. My own attempts to test this using florescent imaging of labeled RNA probes (smFISH) were hindered by low probe signal as well as cell morphology that made imaging and quantification of localization difficult. Probe signal optimization and selection of a well-suited cell type (flat with a large cytoplasm) such as U2OS cells will be key to the success of imaging-based experiments. MERFISH is a similar imaging-based method

for analysis of subcellular RNA localization that could be useful here (Xia et al., 2019). Another possible approach that does not rely on imaging would be to using the recently developed APEX-seq method of proximity-labeling RNA to measure subcellular distributions of mRNA transcripts (Fazal et al., 2019).

How LARP4 achieves its RNA-target specificity remains unresolved. The binding profile of LARP4 across target transcripts often shows a narrow steep peak in density near stop codon or adjacent 3'UTR region with a similar pattern sometimes observed near the start codon. Between the start and stop codons, a broad binding peaks covering most of the coding region are often observed with a density much lower than the primary peak near the stop codon. These distinct patterns in binding profiles suggest a combination of binding mechanisms.

It is possible the steep high density binding sites are generated by direct interaction between LARP4 and target RNAs and the broad lower density binding sites are facilitated through protein-protein interactions of LARP4 with other RBPs or translational proteins. For instance, LARP4's interaction with the ribosome associated protein RACK1 could facilitate the lower density broad binding sites across the protein coding regions of target mRNAs by linking LARP4 to a translating ribosome and dragging LARP4 across the coding region. Future studies could test this hypothesis with a modified eCLIP experiment where cells are treated with a translational terminator such as puromycin or a translational initiation inhibitor prior to UV crosslinking. The expectation would be that puromycin treatment would abolish most binding in the coding regions and translational initiation inhibitor treatment would also abolish most binding in the coding regions away from the start codon with

an increase in binding near the start codon due to ribosomes stalled at the start site. The role of different protein regions of LARP4 plays in RNA-target binding could also be studied by expressing mutant versions of epitope-tagged LARP4 in cells and then performing an eCLIP experiment using the epitope tag to immunoprecipitate the mutant LARP4. For instance, mutations in the RNA-binding regions could test if they are responsible for the steep 3'UTR peaks. Mutation or deletion of the RACK1 interaction region could provide insight into the role of that region in the RNA-target binding of LARP4.

A search for overrepresented linear motifs in the binding sites of LARP4 did not reveal any robust motifs. Future studies could look search for overrepresented motifs in a subset of LARP4 binding sites. For instance, removing the lower density broad binding sites from the analysis might reveal more significantly enriched binding motifs. Another approach would be to focus the analysis on the binding sites within mitochondrial mRNA targets which make up 25-30% of LARP4 total RNA-targets, this may identify a LARP4 motif specific to mitochondrial targets. LARP4 could also interact with structural motifs such as hairpins present in target mRNAs, future studies should test this possibility by using RNA structure prediction methods to look for similar structures in mRNA targets of LARP4.

The effects of LARP4 depletion should also be explored in cell types with physiologies that could exacerbate a reduction protein targeting to mitochondria or have high energy requirements. For example, many immune cell types switch metabolisms rapidly to become more dependent on OXPHOS metabolism in response to cell signaling events (Pearce et al., 2013). Rapid protein targeting to

mitochondria to facilitate increased mitochondrial biosynthesis and OXPHOS function could be important for these cell types. Neurons have high energy demands and are dependent on OXPHOS (Watts et al., 2018). They are also very polarized cells with mitochondria traveling down cell projections far away from the cell body where nuclear-encoded mitochondrial mRNAs are transcribed putting unique demands on protein targeting to mitochondria (Mandal et al., 2019). For these reasons the effect of LARP4 depletion in neurons should explored in future studies.

Portions of Chapter 6 are included in a completed manuscript that has been accepted for review at Cell Reports. “LARP4 Is an RNA-Binding Protein That Binds Nuclear-Encoded Mitochondrial mRNAs To Promote Mitochondrial Function” Lewis, Benjamin; Cho, Chae Yun; Yeo, Gene; Hunter, Tony. The dissertation author was the primary investigator and author of this paper.

# Chapter 7: Experimental procedures and reagents

## 7.1 Experimental procedures

### DNA Constructs

The coding region of the full length LARP4 (isoform A) was amplified from pFLAG-CMV2 plasmid containing a LARP4 expression cassette (gift from the Richard Maraia lab) and cloned into a gateway entry plasmid by Gibson assembly. The LARP4-GFP fusion protein was generated by extension PCR and cloned into an entry plasmid. Subsequently lenti-viral expression plasmids were produced via gateway cloning. CRISPR plasmids were cloned according to Zhang lab protocols (Ran et al. 2013).

### Cell culture and manipulations

All cell lines were maintained in DMEM (Corning,10-013-CV) supplemented with 10% fetal bovine serum at 37 °C with 10% $CO_2$. Cultures were passaged with accutase (Innovative Cell Technologies, AT104) every three days. HEK293 and U2OS cell lines were obtained from ATCC and cultured for 30 passages or less. Periodic testing for mycoplasma was performed. All transfections were performed using lipofectamine 2000 (Thermo-Fisher,11668030) according to the manufacturer's instructions. All transductions were performed using filtered cell culture media from cells transfected with lenti-viral production plasmids.

### CRISPR knockout cell line generation

LARP4 knock cell lines were generated with CRISPR/Cas9 using a two-guide transfection strategy. Cas9 and sgRNA guides were introduced into cells by transfection of plasmids expressing Cas9 and sgRNA guides. Forty-eight hours after

transfection, cells were singularized and sorted into individual wells by flow cytometry to generate subclone cultures. Recovered clones were first screened by PCR using primers flanking the two adjacent CRISPR target site. Clones showing evidence of a deletion in the target region were selected for validation by immunoblot analysis. CRISPR guides sequences and PCR screening primers were used and are contained in the key recourses table. For the knockout clones used in this study, the genomic region flanking the gRNA target site was amplified and cloned into a cloning vector and plasmids from 10 individual transformants for each clone sent for sequencing.

Incucyte cell proliferation assays

For analysis of cell proliferation rates, the Zoom Incucyte live cell imaging device was used to make image-based cell density measurements of cell cultures at regular intervals. The manufacturer's image analysis software was used to calculate either percent well confluency (HEK293) or direct cell counts (U2OS) at each time point. These cell density measurements were used to calculate density doubling times for individual wells of the cell culture plate. For experiments with HEK293 cells 6,000 cells were plated into wells of 96 well plates, 24 hours prior to transfer into the Incucyte device and growth measurements recorded for 4-5 days. Reported confluency doubling times represent averages of three biological replicates, each of which represents an average of technical replicates, which consisted of eight individual wells. For experiments with U2OS cells, cells were first transduced with a lentivirus expressing a nuclear red fluorescent protein to directly track cell counts. For

experiments with U2OS cells only two biological replicates were performed and cell doubling times reported are averages of technical replicates.

Immunoblotting

For standard immunoblot analysis, lysates were prepared in RIPA lysis buffer (Thermo-Fisher,89900) supplemented with EDTA-free complete protease inhibitors (Sigma,5892791001). Protein concentrations determined by the BCA assay (Thermo-Fisher,23227). Sample concentrations were normalized and prepared for PAGE in a reducing loading buffer, depending on the target protein 10-30 µg of protein per sample were resolved through SDS acrylamide gels. Proteins were then transferred onto PVDF membranes (Milipore, IPFL00010) via the wet-transfer procedure. Total protein transferred protein was then quantified using the Revert fluorescent total protein stain (Li-Cor,926-11011) according to the manufacturer's instructions. Membranes were then blocked via a one hour incubation in blocking buffer (150 mM NaCl, 50 mM Tris, pH 7.5, 5% w/v bovine serum album). Primary antibody incubations were carried out for two hours at room temperature in blocking buffer supplemented with 0.1% Tween-20. Secondary antibody incubations were carried out for one hour at room temperature in blocking buffer supplemented with 0.1% Tween-20 and 0.01% SDS. The following primary antibodies were used at 1:1000 dilution unless stated otherwise: (LARP4, Maraia Lab), (NDUFA8, Abcam, ab184952, dilution: 1:20,000), (NDUFB9, Abcam, ab200198, dilution: 1:5,000), (COX5B , Abcam, ab180136, dilution: 1:10,000), (COX6B1, Abcam, ab131277), (MRPS5, Abcam, ab96291), (MRPL24, Santa Cruz Biotechnology, sc-393857, dilution: 1:100),

(NDUFA1, Abcam, ab176563), (ATP5L, Invitrogen, PA5-60783), (Calnexin, Santa Cruz Biotechnology, sc-11397, dilution: 1:100), (TBP, Cell Signaling, 44059), (Anti-puromycin, Millipore, MABE343, dilution: 1:20,000), (Anti-DNP, Millipore, S7150, dilution: 1:150). The following secondary antibodies were used at a 1:20,000 dilution: (Goat anti-rabbit 800 nm, Invitrogen, SA535571), (Goat anti-mouse 800 nm, Invitrogen, SA535521), (Goat anti-rabbit Alexa 680, Invitrogen, A-21109), (Goat anti-mouse Alexa flour 680, Invitrogen, A-21058). After each antibody incubation membranes were washed three times in wash buffer (150m M NaCl, 50 mM Tris, pH 7.5, 0.1% Tween-20 ) for five min. Stained membranes were rinsed in TBS (150mM NaCl, 50mM Tris, pH 7.5) and visualized using the Odyssey imaging system. The LI-COR imaging software was used to quantify both total transferred protein per lane and signal intensity of the target band. All reported immunoblot signal quantifications are the target band signal normalized by the total protein signal of the lane containing the target band.

Oxiblot assay

For analysis of oxidized protein abundance using the Oxiblot assay kit (Millipore, S7150), lysates were prepared in RIPA lysis buffer supplemented with 50 µM DTT. Protein concentrations between samples were normalized and oxidized proteins were then derivatized with DNP according to the manufacturer's instructions. Immunoblotting was then performed and quantified as previously described, using the anti-DNP primary antibody provided with Oxiblot assay kit (Millipore, S7150).

Puromycin incorporation assay

For analysis of translation rates by the puromycin incorporation assay (Schmidt, et al. 2009), cells in culture were incubated in the presence of puromycin (10 µg/ml) for 10 min prior to lysate collection in RIPA buffer. Immunoblotting was then performed and quantified as previously described using an anti-puromycin primary antibody (Millipore, MABE343). Negative control sample cell cultures were processed similarly with the exception that cells were either incubated with unmodified media, or puromycin labeling media supplemented with cycloheximide at a final concentration of 100 µg/ml.

RT-qPCR analysis

For analysis of mRNA abundance, total RNA extracts were collected from cell cultures containing approximately 500,000 cells by directly applying Trizol reagent (Thermo-Fisher, 15596026). Total RNA was further purified using the Direct-zol column purification kit (Zymo, R2050). Reverse transcriptase reactions were carried out using the SuperScript™ III Reverse Transcriptase kit (Invitrogen, 18080044), according to the manufacturer's instructions. A RT-qPCR analysis was then performed on the resulting cDNA with Power SYBR™ Green PCR Master Mix (Thermo-Fisher, 4368577) using primer pairs listed in the key resource table. For each sample type three biological replicates (independent collection days) were assayed, with at least two technical replicates (replicate RT-qPCR reactions) performed for each biological replicate.

mtDNA abundance analysis

For analysis mtDNA abundance, approximately 500,000 cells were collected and pelleted. Cell pellets were then resuspended in 50 mM NaOH and incubated at

95 °C for one hour. Samples were then neutralized with 1 M Tris, pH 8.0 using 1/10$^{th}$ the volume of lysis buffer used. DNA concentration was then estimated by spectrophotometry and qPCR performed using 3 ng of DNA per 10 µl reaction of Power SYBR™ Green PCR Master Mix (Thermo-Fisher, 4368577). For each sample two reactions were prepared using primers targeting either the nuclear DNA (beta-2-microglobulin) or primers targeting the mitochondrial DNA (mitochondrially encoded tRNA leucine 1). The ratio of cT values from the two primer sets was used to estimate the ratio of mitochondrial DNA to nuclear DNA. For each sample type at least three biological replicates (independent collection days) were assayed, with at least two technical replicates (replicate qPCR reactions) performed for each biological replicate.

Magnetic Isolation of mitochondria

Magnetic isolation of mitochondria was performed using the Militenyi Biotec Human Mitochondria Isolation Kit according to the manufacturer's instructions with additional modifications and the following experiment specific details. HEK293 cells were seeded at a density of 15X10^6 per 15 cm plate, 24 hours before collection. Cells were harvested using DPBS and a rubber policeman, approximately 10% of the cells collected were pelleted and set aside to be used as matched whole cell extract samples and the remaining 90% pelleted and resuspend in 1 ml of the kit's lysis buffer, which was supplemented with protease inhibitors (Sigma, 5892791001). A 26-gauge needle and 1 ml syringe were used to homogenize the cell lysates. After optimization, the following protocol was found to be effective for 85-95% cell disruption: 5 strokes of the entire homogenate volume, ice for 60 seconds then

repeat three more times for a total of 20 stroke repetitions. The final pellet for mitochondria extracts and the whole cell extracts were resuspended in RIPA buffer supplemented with protease inhibitors (Sigma, 5892791001). To remove the antibody-conjugated magnetic nanobeads prior analysis by quantitative TMT mass spectrometry, lysed mitochondria extracts were passed over fresh LS columns from the isolation kit, that had been equilibrated with RIPA buffer.

TMT-mass spectrometry and analysis

Samples were precipitated by methanol/ chloroform and redissolved in 8 M urea/100 mM TEAB, pH 8.5. Proteins were reduced with 5 mM tris(2-carboxyethyl-phosphine hydrochloride (TCEP, Sigma-Aldrich) and alkylated with 10 mM chloroacetamide (Sigma-Aldrich). Proteins were digested overnight at 37 $^{o}$C in 2 M urea/100 mM TEAB, pH 8.5, with trypsin (Promega). The digested peptides were labeled with 10-plex TMT (Thermo, 90309), pooled samples were fractionated by basic reversed phase (Thermo, 84868).

The TMT labeled lysate samples were analyzed on a Fusion Lumos mass spectrometer (Thermo). Samples were injected directly onto a 25 cm, 100 μm ID column packed with BEH 1.7 μm C18 resin (Waters). Samples were separated at a flow rate of 300 nL/min on an EasynLC 1200 (Thermo). Buffer A and B were 0.1% formic acid in water and 90% acetonitrile, respectively. A gradient of 1–25% B over 180 min, an increase to 40% B over 30 min, an increase to 100% B over another 20 min and held at 90% B for a 10 min was used for a 240 min total run time. Peptides were eluted directly from the tip of the column and nanosprayed directly into the mass spectrometer by application of 2.8 kV voltage at the back of the column.

The Lumos was operated in a data dependent mode. Full MS1 scans were collected in the Orbitrap at 120k resolution. The cycle time was set to 3 s, and within this 3 s the most abundant ions per scan were selected for CID MS/MS in the ion trap. MS3 analysis with multinotch isolation (SPS3) was utilized for detection of TMT reporter ions at 60k resolution (McAlister et al., 2014). Monoisotopic precursor selection was enabled and dynamic exclusion was used with exclusion duration of 10 s.

Protein and peptide identification were done with Integrated Proteomics Pipeline – IP2 (Integrated Proteomics Applications). Tandem mass spectra were extracted from raw files using RawConverter (He et al., 2015) and searched with ProLuCID (Xu et al., 2015) against Uniprot human database. The search space included all fully-tryptic and half-tryptic peptide candidates. Carbamidomethylation on cysteine and TMT on lysine and peptide N-term were considered as static modifications. Data was searched with 50 ppm precursor ion tolerance and 600 ppm fragment ion tolerance. Identified proteins were filtered to using DTASelect (Tabb et al., 2002) and utilizing a target-decoy database search strategy to control the false discovery rate to 1% at the protein level (Peng et al., 2003). Quantitative analysis of TMT was done with Census (Park et al., 2014) filtering reporter ions with 20 ppm mass tolerance and 0.6 isobaric purity filter.

Protein total intensity on each channel was normalized by the sum of all proteins in the same channel. These normalized intensity values for each replicate (N=4) were averaged together by group (WT or KO) and used to calculate average normalized protein abundance for each protein. These values were used to calculate KO/WT ratios for each protein and determine sets of proteins present in increased or

decreased abundance for gene ontology analysis. Common keratin contaminants were removed manually.

Extracellular flux analysis

Oxygen consumption rates and proton efflux rates were measured using the XF-96 extracellular flux analyzer (Agilent) and XF-96 FluxPaks (Agilent). The mito-stress test (MTS) assay was carried out according to the manufacturer's instructions with additional modifications and the following experiment specific details. Approximately 24 hours prior to assay, cells were seeded onto XF-96 cell culture plates and at a density of 25,000 or 16,000 cells per well for HEK293 cells or U2OS cells respectively. For experiments with HEK293 cells the following final concentrations of small molecules were applied: oligomycin (1.5 μM), CCCP (1.0 μM) Rotenone (0.5 μM) and Antimycin A (0.5 μM). For experiments with U2OS cells the following final concentrations of small molecules were applied: oligomycin (1.0 μM), CCCP (2.0 μM), Rotenone (0.5 μM) and Antimycin A (0.5 μM). The following small molecules required for the MTS assay were ordered individually and 10 mM stocks prepared and stored at -20°C: (CCCP, Sigma, C2920), (Oligomycin, Sigma, O4876), (Antimycin A, Sigma, A8674). The assay media used was XF DMEM base media (Agilent, 103575-100) supplemented with glucose 10 mM, pyruvate 1 mM and glutamine 2 mM. For MTS assay well normalization, DAPI (Thermo-Fisher, D3571) was added to the final small molecule injection solution such that final well concentration was 1 μg/ml. After completion of flux measurements, the cell culture plates were transferred to the Celigo plate cytometer (Cyntellect), DAPI stained nuclei imaged, and direct cell counts for each well made using the Celigo cytometer

software. For analysis of extracellular flux measurements, the Wave Desktop program (Agilent) was used.

Flow Cytometry

For flow cytometry measurements, cells were seeded 24 hours prior to collection at a density of 250,000 cells per well of a 12-well plate. Cells were harvested with accutase, pelleted, and resuspend in flow buffer (DPBS, 2% FBS, 1 µg/ml DNase I, 1 µg/ml DAPI) prior to flow analysis. Cell suspensions were analyzed with a LSR II flow cytometer (BD Biosciences) and data analyzed with FACSDiva software (BD Biosciences). For analysis of mitochondrial membrane potential (MMP), cells were co-stained with the MMP dependent dye, tetramethylrhodamine-methyl-ester-perchlorate (TMRM) (Thermo-Fisher, T668) and the mitochondrial mass dependent dye, MitoTracker™ Green (MTG) (Thermo-Fisher, M7514). MMP measurements were then normalized by the mitochondrial mass dependent dye measurements. For flow cytometry staining, media was replaced with staining media containing TMRM (50 nM) and MTG (50 nM) and cultures incubated at 37 °C for 25 min prior to harvest. To validate membrane potential of TMRM dye, control samples were created by adding either a depolarizing agent (CCCP 30 µM) or a hyperpolarizing agent (oligomycin 10 µM) to the staining media.

seCLIP-library preparation and analysis

For analysis of RNA-targets bound by LARP4 in HEK293 cells, seCLIP experiments were carried as previously described (Van Nostrand et al., 2017) with the following experiment specific details. UV-crosslinked LARP4 was with immunoprecipitated with anti-LARP4 rabbit polyclonal antibody (Bethly, A303-900A).

Libraries were sequenced as 75 base-pair single-end reads on the HiSeq4000 to approximately 20 million reads. Reads were processed through the previously described eCLIP0v0.40 pipeline (Van Nostrand et al., 2017). Input normalized peaks were further filtered by the irreproducible discovery rate (IDR) and merged using merge_peaks-v0.05 ([IDR] https://github.com/YeoLab/merge_peaks).

Gene ontology analysis

For all gene ontology analysis, the Metascape gene ontology method and sever was used (Zho u et al., 2019). From each dataset two gene sets were generated, a set of foreground genes and a background gene set. For analysis of LARP4 eCLIP datasets (HEK293, HepG2 and K562), the set of foreground genes (genes that encode for RNA-targets of LARP4) were generated from the annotated bed file of the merged IDR peaks. Genes with a CLIP peak passing the following filters were included in each set of foreground genes: log2 fold change (CLIP-IP/Input) greater than 4 and -log10(pValue) greater than 7. For background gene sets, the matched CLIP input datasets were used, all genes with at least 5 reads in any exonic region were included in each background set. For analysis of the TMT mass spectrometry datasets foreground gene sets were generated from proteins present in either increased abundance or decreased abundance and background gene sets defined by all proteins detected in each mass spectrometry dataset (Mitochondrial extracts or Whole cell extracts). Proteins with significantly increased abundance were defined as having a log2 fold change (KO/WT) of greater than 0.2 and pValue of less 0.05. Proteins with significantly decreased abundance were

defined as having a log2 fold change (KO/WT) of less than negative 0.2 and pValue of less 0.05.

Statistical analysis

Average values were tested for statistical differences using two-tailed unpaired Student's t-tests unless otherwise stated in the figure legend (Figure 24B). Averages of biological replicates were plotted as mean values ± standard error and replicate number denoted with a capital N. Averages of technical replicates were plotted as mean values ± standard deviation and replicate number denoted with a lowercase n. The statistical significance of differences of averages are indicated by * $p \leq 0.05$, ** $p \leq 0.001$, *** $p \leq 0.0001$, **** $p \leq 0.00001$. Statistical significance of enrichments was determined by the hypergeometric test.

## 7.2 Reagents and oligos

Table 1. List of all key reagents used in this study.

**Key Resource Table**

| Reagent Type | Reagent or Resource | Source or Reference | Identifiers | Additional information |
|---|---|---|---|---|
| Antibody | LARP4 | Maraia Lab | gift | 1:1000 |
| Antibody | LARP4 | Bethly | A303-900A | 1:1000 |
| Antibody | NDUFA8 | Abcam | ab184952 | 1:20,000 |
| Antibody | NDUFB9 | Abcam | ab200198 | 1:5000 |
| Antibody | COX5B | Abcam | ab180136 | 1:10,000 |
| Antibody | COX6B1 | Abcam | ab131277 | 1:1000 |
| Antibody | MRPS5 | Abcam | ab96291 | 1:1000 |
| Antibody | MRPL24 | Santa Cruz Biotechnology | sc-393857 | 1:100 |
| Antibody | ATP5L | Invitrogen | PA5-60783 | 1:1000 |
| Antibody | Calnexin | Santa Cruz Biotechnology | sc-11397 | 1:1000 |
| Antibody | TBP | Cell Singaling | 44059 | 1:1000 |
| Antibody | NDUFA1 | Abcam | ab176563 | 1:1000 |
| Antibody | Anti-puromycin | Milipore | MABE343 | 1:1000 |
| Antibody | Anti-DNP | Milipore | S7150 (kit) | 1:1000 |
| Antibody | Goat anti-rabbit 800nm | Invitrogen | SA535571 | 1:20,000 |
| Antibody | Goat anti-mouse 800nm | Invitrogen | SA535521 | 1:20,000 |
| Antibody | Goat anti-rabbit Alexa flour 680 | Invitrogen | A-21109 | 1:20,000 |
| Antibody | Goat anti-mouse Alexa flour 680 | Invitrogen | A-21058 | 1:20,000 |
| Cell Culture | Seahorse XF DMEM medium | Agilent | 103575-100 | |
| Cell Culture | DMEM | Corning | 10-013-CV | |
| Cell Culture | Accutase | Innovative Cell Technologies | AT104 | |
| Cell Culture | Lipofectamine 2000 | Thermo-Fisher | 11668030 | |
| Assay | RIPA Buffer | Thermo-Fisher | 89900 | |
| Assay | cOmplete™ ULTRA Tablets, Mini, EDTA-free, | Sigma | 5892791001 | |
| Assay | OxyBlot Protein Oxidation Detection Kit | Millipore | S7150 | |

Table 1. List of all key reagents used in this study. Continued.

**Key Resource Table**

| Reagent Type | Reagent or Resource | Source or Reference | Identifiers | Additional information |
|---|---|---|---|---|
| Assay | Power SYBR™ Green PCR Master Mix | Thermo-Fisher | 4368577 | |
| Assay | Human Mitochondria Isolation Kit | Militenyi Biotec | 130-094-532 | |
| Assay | Revert™ 700 Total Protein Stain | Li-Cor | 926-11011 | |
| Assay | Pierce™ BCA Protein Assay Kit | Thermo-Fisher | 23227 | |
| Assay | Immobilon-FL PVDF Membrane | Milipore | IPFL00010 | |
| Assay | Direct-zol RNA Miniprep | Zymo | R2050 | |
| Assay | Trizol | Thermo-Fisher | 15596026 | |
| Assay | SuperScript™ III Reverse Transcriptase | Invitrogen | 18080044 | |
| Chemical | Cycloheximide 100mg/ml | Sigma | C4859 | |
| Chemical | Carbonyl cyanide 4-(trifluoromethoxy)phenylhydrazone | Sigma | C2920 | |
| Chemical | Oligomycin | Sigma | O4876 | |
| Chemical | Antimycin A | Sigma | A8674 | |
| Chemical | Rotenone | Mp Biomedicals Inc | 0215015401 | |
| Chemical | tetramethylrhodamine, methyl ester, perchlorate (TMRM) | Thermo-Fisher | T668 | |
| Chemical | DAPI (4',6-Diamidino-2-Phenylindole, Dilactate) | Thermo-Fisher | D3571 | |
| Chemical | MitoTracker™ Green FM | Thermo-Fisher | M7514 | |

Table 2. List of all oligonucleotides used in this study.

**Oligo Table**

| Oligo ID | Sequence (5' -> 3') | Related Figures | Assay |
|---|---|---|---|
| LARP4 sgRNA-A (F) | CACCGTTGTTCAGTACACTTCGCCA | Fig 14 | CRISPR |
| LARP4 sgRNA-A (R) | aaacTGGCGAAGTGTACTGAACAAC | Fig 14 | CRISPR |
| LARP4 sgRNA-B (F) | CACCGCGACATGTTGCTTTTCGTGG | Fig 14 | CRISPR |
| LARP4 sgRNA-B (R) | aaacCCACGAAAAGCAACATGTCGC | Fig 14 | CRISPR |
| LARP4 KO screen(F) | ACTTTTCGGCAGGGTTGGTTTG | Fig 14 | CRISPR |
| LARP4 KO screen(R) | CCAGAACAGCCCTCCGTTTTTC | Fig 14 | CRISPR |
| NUP85 (ref) (FWD) | AGTGACTCGGCTCTTGTACTC | Fig 18 | cDNA qPCR |
| NUP85 (ref) (REV) | GCGATGCTGCACTCTTTGAT | Fig 18 | cDNA qPCR |
| ACTB (FWD) | CTCTTCCAGCCTTCCTTCCT | Fig 18 | cDNA qPCR |
| ACTB (REV) | AGCACTGTGTTGGCGTACAG | Fig 18 | cDNA qPCR |
| MRPL23 (FWD) | GACAAGGGTGGACCTCAGGAAT | Fig 18 | cDNA qPCR |
| MRPL23 (REV) | CGGCTTCTTGATCCTCACGTTTC | Fig 18 | cDNA qPCR |
| MRPS5 (FWD) | GAAGAGTGTTCTCGGCAATGGC | Fig 18 | cDNA qPCR |
| MRPS5 (REV) | TACTGCTGGCTCATCAGGTGAC | Fig 18 | cDNA qPCR |
| MRPL24 (FWD) | CCATTACCGCTATGGGATGAGC | Fig 18 | cDNA qPCR |
| MRPL24 (REV) | CCACAGAACAGATACCAGTCTTC | Fig 18 | cDNA qPCR |
| MRPL14 (FWD) | ACTGGGAGTCTGAGTGCGATT | Fig 18 | cDNA qPCR |
| MRPL14 (REV) | AGGAGCCCGATGGTATGGG | Fig 18 | cDNA qPCR |
| MRPL51 (FWD) | TCTCTTGGTGTGCCTAGATTGA | Fig 18 | cDNA qPCR |
| MRPL51 (REV) | CACTCCGAACATGGCCCTTTT | Fig 18 | cDNA qPCR |
| MRPL18 (FWD) | GCAGCGAAACCTGAAGTGGA | Fig 18 | cDNA qPCR |
| MRPL18 (REV) | GTGCCAGAACTCACGGGAG | Fig 18 | cDNA qPCR |
| MRPS11 (FWD) | GGGATTTCGGAATGCCAAGAA | Fig 18 | cDNA qPCR |
| MRPS11 (REV) | GGATCACGCCCTTTTGTTTAGC | Fig 18 | cDNA qPCR |
| MRPS34 (FWD) | CTCCGGGCCATGATTATCGC | Fig 18 | cDNA qPCR |
| MRPS34 (REV) | CCATGCGTATCCTCTGCACAT | Fig 18 | cDNA qPCR |
| MRPS6 (FWD) | GGCCAGAGACTGCTGCTAC | Fig 18 | cDNA qPCR |
| MRPS6 (REV) | GCGGTGGGTGCATAAAAATCC | Fig 18 | cDNA qPCR |
| NDUFB7 (FWD) | TGCGCATGAAGGAGTTTGAG | Fig 18 | cDNA qPCR |
| NDUFB7 (REV) | CAGATTTGCCGCCTTCTTCTC | Fig 18 | cDNA qPCR |

Table 2. List of all oligonucleotides used in this study. Continued.

**Oligo Table**

| Oligo ID | Sequence (5' -> 3') | Related Figures | Assay |
|---|---|---|---|
| NDUFS1 (FWD) | TCGGATGACTAGTGGTGTTA | Fig 18 | cDNA qPCR |
| NDUFS1 (REV) | TTATAGCCAAGGTCCAAAGC | Fig 18 | cDNA qPCR |
| NDUFS6 (FWD) | TTCGGTTTGTAGGTCGTCAGA | Fig 18 | cDNA qPCR |
| NDUFS6 (REV) | CCATCGCACGCTATCACCC | Fig 18 | cDNA qPCR |
| NDUFB11 (FWD) | CGTCCGCTGGGAATCTAGC | Fig 18 | cDNA qPCR |
| NDUFB11 (REV) | ACGGGGTCCTTGTCATAACCA | Fig 18 | cDNA qPCR |
| NDUFA8 (FWD) | CCCAACAAGGAGTTTATGCTCT | Fig 18 | cDNA qPCR |
| NDUFA8 (REV) | CACAGTGACGTTTTATCTGCCT | Fig 18 | cDNA qPCR |
| NDUFB9 (FWD) | GTGGTGCGTCCAGAGAGAC | Fig 18 | cDNA qPCR |
| NDUFB9 (REV) | GGCCTTCGCCATATCCTTTTC | Fig 18 | cDNA qPCR |
| UQCRQ (FWD) | ATCCGCACGTCTTCACTAAAG | Fig 18 | cDNA qPCR |
| UQCRQ (REV) | TGGATCTCTCGAACTCTTCAGTC | Fig 18 | cDNA qPCR |
| COX5B (FWD) | CATCTGGAGGTGGTGTTC | Fig 18 | cDNA qPCR |
| COX5B (REV) | CTTGTAATGGGCTCCACA | Fig 18 | cDNA qPCR |
| COX7A2 (FWD) | CTCGGAGGTAGTTCCGGTTC | Fig 18 | cDNA qPCR |
| COX7A2 (REV) | TCTGCCCAATCTGACGAAGAG | Fig 18 | cDNA qPCR |
| COX15 (FWD) | AGTCTGGCCTCTCGATGGTAG | Fig 18 | cDNA qPCR |
| COX15 (REV) | ACCCCACATTCGGTGTGAGTA | Fig 18 | cDNA qPCR |
| COX6B1 (FWD) | CTACAAGACCGCCCCTTTTGA | Fig 18 | cDNA qPCR |
| COX6B1 (REV) | GCAGAGGGACTGGTACACAC | Fig 18 | cDNA qPCR |
| ATP5G1 (FWD) | TTCCAGACCAGTGTTGTCTCC | Fig 18 | cDNA qPCR |
| ATP5G1 (REV) | GACGGGTTCCTGGCATAGC | Fig 18 | cDNA qPCR |
| ATP5L (FWD) | ATGGCCCAATTTGTCCGTAAC | Fig 18 | cDNA qPCR |
| ATP5L (REV) | TGGCGTAGTACCAAAATGTGG | Fig 18 | cDNA qPCR |
| MITO-tRNA (FWD) | CACCCAAGAACAGGGTTTGT | Fig 30D | mtDNA qPCR |
| MITO-tRNA (REV) | TGGCCATGGGTATGTTGTTA | Fig 30D | mtDNA qPCR |
| B2M (FWD) | TGCTGTCTCCATGTTTGATGTATCT | Fig 30D | mtDNA qPCR |
| B2M (REV) | TCTCTGCTCCCCACCTCTAAGT | Fig 30D | mtDNA qPCR |

Portions of Chapter 7 are included in a completed manuscript that has been accepted for review at Cell Reports. “LARP4 Is an RNA-Binding Protein That Binds Nuclear-Encoded Mitochondrial mRNAs To Promote Mitochondrial Function” Lewis, Benjamin; Cho, Chae Yun; Yeo, Gene; Hunter, Tony. The dissertation author was the primary investigator and author of this paper.

References

Adams, D. R., Ron, D., & Kiely, P. A. (2011). RACK1, A multifaceted scaffolding protein: Structure and function. *Cell Communication and Signaling : CCS*, *9*(1), 22–22. https://doi.org/10.1186/1478-811x-9-22

Balaban, R. S., Nemoto, S., & Finkel, T. (2005). Mitochondria, Oxidants, and Aging. *Cell*, *120*(4), 483–495. https://doi.org/10.1016/j.cell.2005.02.001

Béthune, J., Jansen, R.-P., Feldbrügge, M., & Zarnack, K. (2019). Membrane-Associated RNA-Binding Proteins Orchestrate Organelle-Coupled Translation. *Trends in Cell Biology*, *29*(2), 178–188. https://doi.org/10.1016/j.tcb.2018.10.005

Birsoy, K., Wang, T., Chen, W. W., Freinkman, E., Abu-Remaileh, M., & Sabatini, D. M. (2015). An Essential Role of the Mitochondrial Electron Transport Chain in Cell Proliferation Is to Enable Aspartate Synthesis. *Cell*, *162*(3), 540–551. https://doi.org/10.1016/j.cell.2015.07.016

Bolender, N., Sickmann, A., Wagner, R., Meisinger, C., & Pfanner, N. (2008). Multiple pathways for sorting mitochondrial precursor proteins. *EMBO Reports*, *9*(1), 42–49. https://doi.org/10.1038/sj.embor.7401126

Boos, F., Labbadia, J., & Herrmann, J. M. (2019). How the Mitoprotein-Induced Stress Response Safeguards the Cytosol: A Unified View. *Trends in Cell Biology*, *30*(3), 241–254. https://doi.org/10.1016/j.tcb.2019.12.003

Bousquet-Antonelli, C., & Deragon, J.-M. (2009). A comprehensive analysis of the La-motif protein superfamily. *RNA*, *15*(5), 750–764. https://doi.org/10.1261/rna.1478709

Bykov, Y. S., Rapaport, D., Herrmann, J. M., & Schuldiner, M. (2020). Cytosolic Events in the Biogenesis of Mitochondrial Proteins. *Trends in Biochemical Sciences*, *45*(8), 650–667. https://doi.org/10.1016/j.tibs.2020.04.001

Carlucci, A., Lignitto, L., & Feliciello, A. (2008). Control of mitochondria dynamics and oxidative metabolism by cAMP, AKAPs and the proteasome. *Trends in Cell Biology*, *18*(12), 604–613. https://doi.org/10.1016/j.tcb.2008.09.006

Cruz-Gallardo, I., Martino, L., Kelly, G., Atkinson, R. A., Trotta, R., Tito, S. D., Coleman, P., Ahdash, Z., Gu, Y., Bui, T. T. T., & Conte, M. R. (2019). LARP4A recognizes polyA RNA via a novel binding mechanism mediated by disordered regions and involving the PAM2w motif, revealing interplay between PABP, LARP4A and mRNA. *Nucleic Acids Research*, *47*(8), 4272–4291. https://doi.org/10.1093/nar/gkz144

Eliyahu, E., Pnueli, L., Melamed, D., Scherrer, T., Gerber, A. P., Pines, O., Rapaport, D., & Arava, Y. (2010). Tom20 Mediates Localization of mRNAs to Mitochondria in a Translation-Dependent Manner ▿ †. *Molecular and Cellular Biology*, *30*(1), 284–294. https://doi.org/10.1128/mcb.00651-09

Fallaize, D., Chin, L.-S., & Li, L. (2015). Differential submitochondrial localization of PINK1 as a molecular switch for mediating distinct mitochondrial signaling pathways. *Cellular Signalling*, *27*(12), 2543–2554. https://doi.org/10.1016/j.cellsig.2015.09.020

Fazal, F. M., Han, S., Parker, K. R., Kaewsapsak, P., Xu, J., Boettiger, A. N., Chang, H. Y., & Ting, A. Y. (2019). Atlas of Subcellular RNA Localization Revealed by APEX-Seq. *Cell*, *178*(2), 473-490.e26. https://doi.org/10.1016/j.cell.2019.05.027

Gabrovsek, L., Collins, K. B., Aggarwal, S., Saunders, L. M., Lau, H.-T., Suh, D., Sancak, Y., Trapnell, C., Ong, S.-E., Smith, F. D., & Scott, J. D. (2020). A-kinase-anchoring protein 1 (dAKAP1)-based signaling complexes coordinate local protein synthesis at the mitochondrial surface. *Journal of Biological Chemistry*, *295*(31), 10749–10765. https://doi.org/10.1074/jbc.ra120.013454

Gao, J., Schatton, D., Martinelli, P., Hansen, H., Pla-Martin, D., Barth, E., Becker, C., Altmueller, J., Frommolt, P., Sardiello, M., & Rugarli, E. I. (2014). CLUH regulates mitochondrial biogenesis by binding mRNAs of nuclear-encoded mitochondrial proteins. *The Journal of Cell Biology*, *207*(2), 213–223. https://doi.org/10.1083/jcb.201403129

García-Rodríguez, L. J., Gay, A. C., & Pon, L. A. (2007). Puf3p, a Pumilio family RNA binding protein, localizes to mitochondria and regulates mitochondrial biogenesis and motility in budding yeast. *The Journal of Cell Biology*, *176*(2), 197–207. https://doi.org/10.1083/jcb.200606054

Gehrke, S., Wu, Z., Klinkenberg, M., Sun, Y., Auburger, G., Guo, S., & Lu, B. (2015). PINK1 and Parkin Control Localized Translation of Respiratory Chain Component mRNAs on Mitochondria Outer Membrane. *Cell Metabolism*, *21*(1), 95–108. https://doi.org/10.1016/j.cmet.2014.12.007

Gerber, A. P., Eddy, S., Herschlag, D., & Brown, P. O. (2004). Extensive Association of Functionally and Cytotopically Related mRNAs with Puf Family RNA-Binding Proteins in Yeast. *PLoS Biology*, *2*(3), e79-13. https://doi.org/10.1371/journal.pbio.0020079

Ginsberg, M. D., Feliciello, A., Jones, J. K., Avvedimento, E. V., & Gottesman, M. E. (2003). PKA-dependent Binding of mRNA to the Mitochondrial AKAP121 Protein. *Journal of Molecular Biology*, *327*(4), 885–897. https://doi.org/10.1016/s0022-2836(03)00173-6

Gray, M. W., Burger, G., & Lang, B. F. (2001). The origin and early evolution of mitochondria. *Genome Biology*, *2*(6), reviews1018.1-reviews1018.5. https://doi.org/10.1186/gb-2001-2-6-reviews1018

He, L., Diedrich, J., Chu, Y.-Y., & Yates, J. R. (2015). Extracting Accurate Precursor Information for Tandem Mass Spectra by RawConverter. *Analytical Chemistry*, *87*(22), 11361–11367. https://doi.org/10.1021/acs.analchem.5b02721

Jackson, J. S., Houshmandi, S. S., Leban, F. L., & Olivas, W. M. (2004). Recruitment of the Puf3 protein to its mRNA target for regulation of mRNA decay in yeast. *RNA*, *10*(10), 1625–1636. https://doi.org/10.1261/rna.7270204

Kamenova, I., Mukherjee, P., Conic, S., Mueller, F., El-Saafin, F., Bardot, P., Garnier, J.-M., Dembele, D., Capponi, S., Timmers, H. T. M., Vincent, S. D., & Tora, L. (2019). Co-translational assembly of mammalian nuclear multisubunit complexes. *Nature Communications*, *10*(1), 1740. https://doi.org/10.1038/s41467-019-09749-y

Keil, M., Bareth, B., Woellhaf, M. W., Peleh, V., Prestele, M., Rehling, P., & Herrmann, J. M. (2012). Oxa1-Ribosome Complexes Coordinate the Assembly of Cytochrome c Oxidase in Mitochondria. *Journal of Biological Chemistry*, *287*(41), 34484–34493. https://doi.org/10.1074/jbc.m112.382630

MacKenzie, J. A., & Payne, R. M. (2007). Mitochondrial protein import and human health and disease. *Biochimica et Biophysica Acta (BBA) - Molecular Basis of Disease*, *1772*(5), 509–523. https://doi.org/10.1016/j.bbadis.2006.12.002

Mandal, A., & Drerup, C. M. (2019). Axonal Transport and Mitochondrial Function in Neurons. *Frontiers in Cellular Neuroscience*, *13*, 373. https://doi.org/10.3389/fncel.2019.00373

Maraia, R. J., Mattijssen, S., Cruz-Gallardo, I., & Conte, M. R. (2017). The La and related RNA-binding proteins (LARPs): structures, functions, and evolving perspectives. *Wiley Interdisciplinary Reviews: RNA*, *15*(12), e1430-43. https://doi.org/10.1002/wrna.1430

Markmiller, S., Soltanieh, S., Server, K. L., Mak, R., Jin, W., Fang, M. Y., Luo, E.-C., Krach, F., Yang, D., Sen, A., Fulzele, A., Wozniak, J. M., Gonzalez, D. J., Kankel, M. W., Gao, F.-B., Bennett, E. J., Lécuyer, E., & Yeo, G. W. (2018). Context-Dependent and Disease-Specific Diversity in Protein Interactions within Stress Granules. *CELL*, *172*(3), 590-598.e13. https://doi.org/10.1016/j.cell.2017.12.032

Mattijssen, S., Iben, J. R., Li, T., Coon, S. L., & Maraia, R. J. (2020). Single molecule poly(A) tail-seq shows LARP4 opposes deadenylation through mRNA lifespan with most impact on short tails. *eLife*, *9*, e59186. https://doi.org/10.7554/elife.59186

McAlister, G. C., Nusinow, D. P., Jedrychowski, M. P., Wühr, M., Huttlin, E. L., Erickson, B. K., Rad, R., Haas, W., & Gygi, S. P. (2014). MultiNotch MS3 Enables Accurate, Sensitive, and Multiplexed Detection of Differential Expression across Cancer Cell Line Proteomes. *Analytical Chemistry*, *86*(14), 7150–7158. https://doi.org/10.1021/ac502040v

Nostrand, E. L. V., Nguyen, T. B., Gelboin-Burkhart, C., Wang, R., Blue, S. M., Pratt, G. A., Louie, A. L., & Yeo, G. W. (2017). Robust, cost-effective profiling of RNA binding protein targets with single-end crosslinking and immunoprecipitation (seCLIP). *Methods in Molecular Biology*, *1648*, 177–200. https://doi.org/10.1007/978-1-4939-7204-3_14

Nostrand, E. L. V., Pratt, G. A., Yee, B. A., Wheeler, E. C., Blue, S. M., Mueller, J., Park, S. S., Garcia, K. E., Gelboin-Burkhart, C., Nguyen, T. B., Rabano, I., Stanton, R., Sundararaman, B., Wang, R., Fu, X.-D., Graveley, B. R., & Yeo, G. W. (2020). Principles of RNA processing from analysis of enhanced CLIP maps for 150 RNA binding proteins. *Genome Biology*, *21*(1), 90. https://doi.org/10.1186/s13059-020-01982-9

Olivas, W., & Parker, R. (2000). The Puf3 protein is a transcript-specific regulator of mRNA degradation in yeast. *The EMBO Journal*, *19*(23), 6602–6611. https://doi.org/10.1093/emboj/19.23.6602

Park, S. K. R., Aslanian, A., McClatchy, D. B., Han, X., Shah, H., Singh, M., Rauniyar, N., Moresco, J. J., Pinto, A. F. M., Diedrich, J. K., Delahunty, C., & Yates, J. R. (2014). Census 2: isobaric labeling data analysis. *Bioinformatics*, *30*(15), 2208–2209. https://doi.org/10.1093/bioinformatics/btu151

Pearce, E. L., & Pearce, E. J. (2013). Metabolic Pathways in Immune Cell Activation and Quiescence. *Immunity*, *38*(4), 633–643. https://doi.org/10.1016/j.immuni.2013.04.005

Peng, J., Elias, J. E., Thoreen, C. C., Licklider, L. J., & Gygi, S. P. (2003). Evaluation of Multidimensional Chromatography Coupled with Tandem Mass Spectrometry (LC/LC−MS/MS) for Large-Scale Protein Analysis: The Yeast Proteome. *Journal of Proteome Research*, *2*(1), 43–50. https://doi.org/10.1021/pr025556v

Quenault, T., Lithgow, T., & Traven, A. (2011). PUF proteins: repression, activation and mRNA localization. *Trends in Cell Biology*, *21*(2), 104–112. https://doi.org/10.1016/j.tcb.2010.09.013

Ran, F. A., Hsu, P. D., Wright, J., Agarwala, V., Scott, D. A., & Zhang, F. (2013). Genome engineering using the CRISPR-Cas9 system. *Nature Protocols*, *8*(11), 2281–2308. https://doi.org/10.1038/nprot.2013.143

Rawat, S., Anusha, V., Jha, M., Sreedurgalakshmi, K., & Raychaudhuri, S. (2019). Aggregation of Respiratory Complex Subunits Marks the Onset of Proteotoxicity in Proteasome Inhibited Cells. *Journal of Molecular Biology*, *431*(5), 996–1015. https://doi.org/10.1016/j.jmb.2019.01.022

Saint-Georges, Y., Garcia, M., Delaveau, T., Jourdren, L., Crom, S. L., Lemoine, S., Tanty, V., Devaux, F., & Jacq, C. (2008). Yeast Mitochondrial Biogenesis: A Role for the PUF RNA-Binding Protein Puf3p in mRNA Localization. *PLoS ONE*, *3*(6), e2293. https://doi.org/10.1371/journal.pone.0002293

Schmidt, E. K., Clavarino, G., Ceppi, M., & Pierre, P. (2009). SUnSET, a nonradioactive method to monitor protein synthesis. *Nature Methods*, *6*(4), 275–277. https://doi.org/10.1038/nmeth.1314

Schwarz, A., & Beck, M. (2019). The Benefits of Cotranslational Assembly: A Structural Perspective. *Trends in Cell Biology*, *29*(10), 791–803. https://doi.org/10.1016/j.tcb.2019.07.006

Sen, A., & Cox, R. T. (2016). Clueless is a conserved ribonucleoprotein that binds the ribosome at the mitochondrial outer membrane. *Biology Open*, *5*(2), 195–203. https://doi.org/10.1242/bio.015313

Sullivan, L. B., Gui, D. Y., Hosios, A. M., Bush, L. N., Freinkman, E., & Vander Heiden, M. G. (2015). Supporting Aspartate Biosynthesis Is an Essential Function of Respiration in Proliferating Cells. *Cell*, *162*(3), 552–563. https://doi.org/10.1016/j.cell.2015.07.017

Tabb, D. L., McDonald, W. H., & Yates, J. R. (2002). DTASelect and Contrast: Tools for Assembling and Comparing Protein Identifications from Shotgun Proteomics. *Journal of Proteome Research*, *1*(1), 21–26. https://doi.org/10.1021/pr015504q

Taggart, J. C., Zauber, H., Selbach, M., Li, G.-W., & McShane, E. (2020). Keeping the Proportions of Protein Complex Components in Check. *Cell Systems*, *10*(2), 125–132. https://doi.org/10.1016/j.cels.2020.01.004

Watts, M. E., Pocock, R., & Claudianos, C. (2018). Brain Energy and Oxygen Metabolism: Emerging Role in Normal Function and Disease. *Frontiers in Molecular Neuroscience*, *11*, 216. https://doi.org/10.3389/fnmol.2018.00216

Williams, C. C., Jan, C. H., & Weissman, J. S. (2014). Targeting and plasticity of mitochondrial proteins revealed by proximity-specific ribosome profiling. *Science*, *346*(6210), 748–751. https://doi.org/10.1126/science.1257522

Wrobel, L., Topf, U., Bragoszewski, P., Wiese, S., Sztolsztener, M. E., Oeljeklaus, S., Varabyova, A., Lirski, M., Chroscicki, P., Mroczek, S., Januszewicz, E., Dziembowski,

A., Koblowska, M., Warscheid, B., & Chacinska, A. (2015). Mistargeted mitochondrial proteins activate a proteostatic response in the cytosol. *Nature*, *524*(7566), 485–488. https://doi.org/10.1038/nature14951

Xia, C., Fan, J., Emanuel, G., Hao, J., & Zhuang, X. (2019). Spatial transcriptome profiling by MERFISH reveals subcellular RNA compartmentalization and cell cycle-dependent gene expression. *Proceedings of the National Academy of Sciences of the United States of America*, *116*(39), 19490–19499. https://doi.org/10.1073/pnas.1912459116

Xu, T., Park, S. K., Venable, J. D., Wohlschlegel, J. A., Diedrich, J. K., Cociorva, D., Lu, B., Liao, L., Hewel, J., Han, X., Wong, C. C. L., Fonslow, B., Delahunty, C., Gao, Y., Shah, H., & Yates, J. R. (2015). ProLuCID: An improved SEQUEST-like algorithm with enhanced sensitivity and specificity. *Journal of Proteomics*, *129*, 16–24. https://doi.org/10.1016/j.jprot.2015.07.001

Yang, R., Gaidamakov, S. A., Xie, J., Lee, J., Martino, L., Kozlov, G., Crawford, A. K., Russo, A. N., Conte, M. R., Gehring, K., & Maraia, R. J. (2011). La-Related Protein 4 Binds Poly(A), Interacts with the Poly(A)-Binding Protein MLLE Domain via a Variant PAM2w Motif, and Can Promote mRNA Stability†. *Molecular and Cellular Biology*, *31*(3), 542–556. https://doi.org/10.1128/mcb.01162-10

Yoo, Y. A., Kim, M. J., Park, J. K., Chung, Y. M., Lee, J. H., Chi, S.-G., Kim, J. S., & Yoo, Y. D. (2005). Mitochondrial Ribosomal Protein L41 Suppresses Cell Growth in Association with p53 and p27Kip1. *Molecular and Cellular Biology*, *25*(15), 6603–6616. https://doi.org/10.1128/mcb.25.15.6603-6616.2005

Zhang, X., Zink, F., Hezel, F., Vogt, J., Wachter, U., Wepler, M., Loconte, M., Kranz, C., Hellmann, A., Mizaikoff, B., Radermacher, P., & Hartmann, C. (2020). Metabolic substrate utilization in stress-induced immune cells. *Intensive Care Medicine Experimental*, *8*(Suppl 1), 28. https://doi.org/10.1186/s40635-020-00316-0

Zhou, Y., Zhou, B., Pache, L., Chang, M., Khodabakhshi, A. H., Tanaseichuk, O., Benner, C., & Chanda, S. K. (2019). Metascape provides a biologist-oriented resource for the analysis of systems-level datasets. *Nature Communications*, *10*(1), 1523. https://doi.org/10.1038/s41467-019-09234-6